



---

UNIVERSITÀ  
DEGLI STUDI  
DI BRESCIA

DOTTORATO DI RICERCA IN PRECISION MEDICINE

---

settore scientifico disciplinare BIO/14 FARMACOLOGIA

CICLO  
XXXV

Carcinoma of the human adrenal cortex:  
identification and in vitro and in vivo study of  
molecular alterations as potential therapeutic targets

PhD Student: Mariangela Tamburello

SUPERVISOR: Sandra Sigala

## Abstract

Il carcinoma della corticale del surrene (AdrenoCortical Carcinoma, ACC) è una rara neoplasia maligna, con una sopravvivenza a 5 anni inferiore al 50% o al 15%, a seconda dello stadio. Il trattamento proposto prevede l'uso di mitotano da solo o in combinazione con la chemioterapia EDP (etoposide, doxorubicina e cisplatino). In alcuni casi, anche la chirurgia e/o radioterapia. Tuttavia, la progressione della malattia si verifica quasi inevitabilmente dopo meno di 18 mesi e non ci sono attualmente linee guida condivise di trattamento.

È necessario quindi identificare nuove strategie terapeutiche. Abbiamo focalizzato la nostra attenzione sui recettori del progesterone (Pg/ PgR), sui recettori degli estrogeni (E/ER), sulla chinasi WEE1, e sul pathway mediato dai recettori del fattore di crescita dei fibroblasti (FGF/FGFR), cercando di dimostrare se la modulazione della loro attività possa esercitare effetti antiproliferativi nei diversi modelli cellulari sperimentali di ACC ora disponibili.

Abbiamo dimostrato che, sebbene l'espressione di ER sia relativamente bassa, il tamoxifene esercita un effetto citotossico sulla linea cellulare NCI-H295R derivante da un tumore primitivo ma non sulle linee metastatiche che esprimono livelli molto bassi di ER. Allo stesso modo, ER è debolmente espresso nei tessuti di ACC e sembra diminuire con la progressione della malattia. Di maggiore interesse sono invece i risultati riguardanti l'effetto citotossico esercitato dal Pg, sebbene con una potenza inferiore nelle linee metastatiche rispetto alle cellule NCI-H295R, probabilmente a causa di una minore espressione dei PgR. L'autofagia e l'apoptosi si verificano gerarchicamente o indipendentemente per contribuire alla morte cellulare indotta dal Pg. Inoltre, gli esperimenti di sospensione del trattamento hanno mostrato che l'effetto del Pg è duraturo nei modelli metastatici. Nel modello zebrafish, Pg ha ridotto significativamente l'area della massa tumorale iniettata con ciascuna linea cellulare di ACC, e la formazione di metastasi negli embrioni iniettati con cellule MUC-1, confermando i risultati in vitro. Questo fenomeno è mediato almeno in parte, dalla riduzione dei livelli e dell'attività di MMP2.

Riguardo WEE1, i nostri risultati hanno mostrato che questa chinasi è maggiormente espressa nei tessuti di ACC e che bassi livelli di WEE1 sono associati a una migliore sopravvivenza globale. È interessante notare che la colorazione nucleare di WEE1 è significativamente più alta nei campioni con mutazioni note in TP53 rispetto a quelli wild type. L'esposizione delle cellule NCI-H295R, JIL-2266 e CU-ACC2 all'inibitore di WEE1, adavosertib, ha indotto la citotossicità con valori di IC50 rispettivamente di 1.17, 1.35 e 0.4  $\mu$ M. Le cellule CU-ACC1 e MUC-1 hanno mostrato una minore sensibilità per adavosertib da solo, ma il suo effetto è stato migliorato se combinato con il cisplatino o la gemcitabina. Questo effetto additivo/sinergico è stato osservato in tutte le linee cellulari.

Infine, abbiamo scelto di valutare il potenziale terapeutico della via FGF/FGFR in ACC poiché diversi studi hanno dimostrato che FGFR1 e FGFR4 sono overespressi negli ACC e che la loro alta espressione è significativamente associata a una prognosi peggiore. L'esposizione delle cellule di ACC a concentrazioni crescenti di tre differenti inibitori degli FGFR erdafitinib, rogaratinib e fisogatinib, ha indotto un effetto citotossico a seconda della linea cellulare, e correlato con l'espressione dei recettori. In conclusione, questi risultati rafforzano il possibile ruolo del Pg nell'ACC; questa ipotesi è al momento l'oggetto dello studio clinico PESETA. Inoltre, la speranza è che i progetti in corso, riguardanti l'uso dell'inibitore di WEE1 adavosertib e degli inibitori degli FGFR, generino risultati solidi che possano fornire la base per futuri studi clinici.

# Summary

|  |    |
|--|----|
| 1. The adrenal gland .....   | 5  |
| 1.1 Structure .....  | 5  |
| 1.2 Development .....  | 6  |
| 1.3 Function .....   | 6  |
| 1.4 Steroid hormone synthesis .....  | 7  |
| 1.5 Adrenal gland tumors .....   | 8  |
| 2. Adrenocortical carcinoma (ACC).....   | 10 |
| 2.1 Epidemiology .....   | 10 |
| 2.2 Clinical presentation .....  | 10 |
| 2.3 Pathogenesis and genetics .....  | 10 |
| 2.4 General prognosis.....   | 13 |
| 2.5 Diagnosis.....   | 13 |
| 2.6 Treatment .....  | 13 |
| 3. Possible therapeutic targets in ACC .....   | 15 |
| 3.1 Progesterone receptors and estrogen receptors .....  | 15 |
| 3.2. WEE1.....   | 17 |
| 3.3 FGF/ FGFR pathway .....  | 18 |
| 4. Aim of the project.....   | 22 |
| 5. Materials and methods .....   | 23 |
| 6. Results .....   | 34 |
| 6.1 Results Part I: assessing the potential of estrogen, progesterone and their receptors in ACC ..... | 34 |
| 6.2 Results Part II: Potential role of WEE1 inhibitor in ACC .....                                     | 49 |
| 6.3 Results Part III: potential role of FGF/FGFR pathway in ACC.....                                   | 53 |
| 7. Discussion .....  | 56 |
| 8. Conclusion .....  | 63 |
| 9. References.....   | 64 |

# 1. The adrenal gland

## 1.1 Structure

The adrenal glands represent a complex endocrine tissue that mediate the body homeostasis and are two retroperitoneal structures lying superomedial to both kidneys. Each gland consists of two functionally distinct part: outer cortex and an inner medulla. [1].

The cortex is surrounded on the outside by a thick capsule consisting of connective tissue and has 3 distinct functional and histological zones: the zona glomerulosa (outermost layer, 15% of cortex), which is composed of ovoid cells forming rosettes similar to glomeruli, then the zona fasciculata (middle layer, 75% of cortex) with its cells in radial cords that constitutes a major part of the gland, and the zona reticularis (innermost layer, 10% of the cortex), which is formed of cords of cells scattered in different directions [2-4].

The adrenal medulla is located at the center of the gland, and it consists of irregularly shaped cells grouped around blood vessels that are modified postganglionic neurons, and preganglionic autonomic nerve fibers lead to them directly from the central nervous system [5, 6]. (Figure 1)

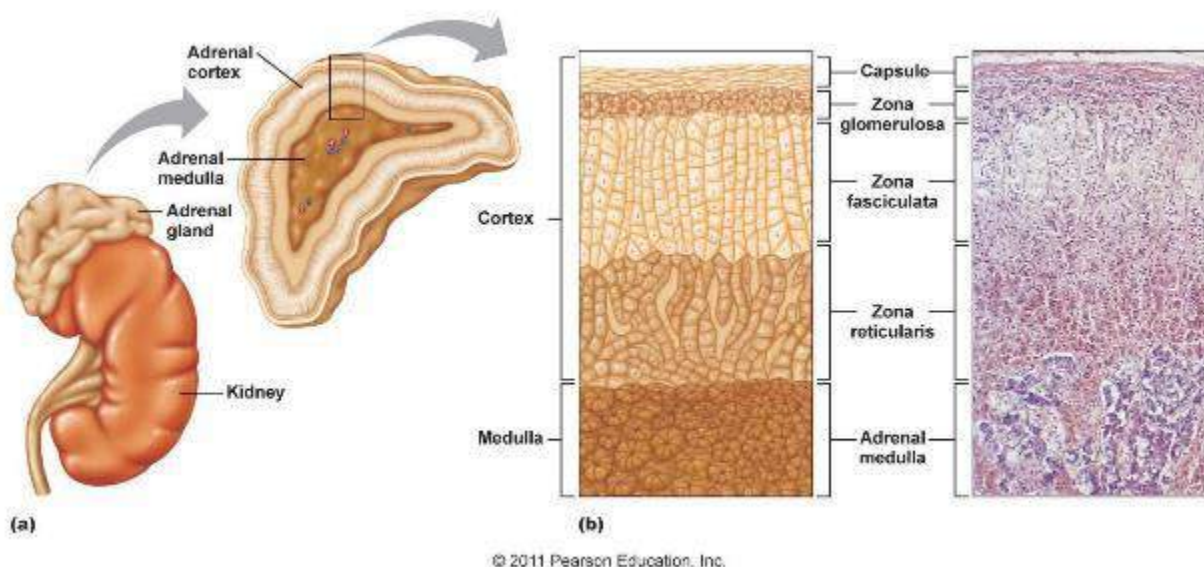


Figure 1. Schematic of the structure and zonation of the adrenal gland. (Pearson Education, 2011).

## 1.2 Development

The adrenal cortex is derived from mesoderm and begins posteromedial to the urogenital ridge. The adrenal medulla is derived from neural crest cells originate from the dorsal aorta. Clusters of chromaffin cells become the distinct medulla after birth. The adrenal gland first appears 28-30 days post-conception. Its development is mediated by steroidogenic factor 1 (SF1), Cbp/p300-interacting transactivator 2 (CITED-2),  $\beta$ -catenin, and others [7-9]. In the 5th week of development, an isolated cluster of cells emerges within the urogenital ridge, identified as the adrenal-gonadal primordial germ cells. Mesothelial cells penetrate the mesenchymal layer and form the fetal adrenal cortex. [10].

The fetal adrenal cortex has a completely different structure than the adult cortex. The human fetal adrenal is one of the largest organs at term (nearly the size of the kidney). The fetal zone is composed of large steroidogenic cells that produce large amounts of the sex hormone dehydroepiandrosterone (DHEA) which is then converted by the placenta to estrogens for the maintenance of normal pregnancy. By the 8th week of gestation, newly formed adrenocortical cells emerge between the capsule and fetal zone, creating the definitive zone, formed of smaller cells that continue to differentiate and later develop into the adult cortex [9, 11]. In the meantime, neural crest cells formed at the apex of the neural folds migrate into the adrenal primordium via a ventral pathway, and then differentiate into chromaffin cells centrally arranged in cords and masses. The cortex engulfs and gradually encapsulates the whole medulla in the later stages of embryonic development [8, 10].

## 1.3 Function

The adrenal gland is a key component of the body's stress system which is composed of the hypothalamic-pituitary-adrenal axis and the sympathetic-adrenal medullary system. It integrates two embryonically distinct endocrine systems within one organ capsule, the steroid hormone-producing cortex and the catecholamine-producing medulla [1, 5]. Adrenal cortex function is mostly regulated by the adrenocorticotrophic hormone (ACTH), produced in the pituitary gland [12], whereas the adrenal medulla releases high levels of catecholamines in response to the activated sympathetic nervous system (SNS) [6].

- The zona glomerulosa of the adrenal cortex is responsible for the synthesis of mineralocorticoids, of which the most important is aldosterone. As part of the renin-angiotensin system, aldosterone is involved in the regulation of plasma sodium ( $\text{Na}^+$ ) and

extracellular potassium (K<sup>+</sup>) levels, thereby controlling electrolyte balance and arterial blood pressure [13].

- The zona fasciculata produces glucocorticoids, of which the predominant hormone is cortisol. This hormone plays a role in the regulation of blood sugar via gluconeogenesis. Cortisol also modulates the immune system and modulates the metabolism of fat, protein, and carbohydrates [14].
- The zona reticularis produces androgens and plays a role in the development of secondary sexual characteristics. The primary androgen produced in the zona reticularis is DHEA, which is the most abundant hormone in the body. It serves as a precursor for the synthesis of many other hormones produced by the adrenal gland, gonads and peripheral tissue, such as progesterone, estrogen, cortisol, and testosterone [15].
- The adrenal medulla synthesizes catecholamines. Catecholamines are made from the precursor of dopamine and combined with tyrosine, thus resulting in norepinephrine. Once norepinephrine has been created, it is then methylated via phenylethanolamine N-methyltransferase (PNMT), which is only present in the adrenal medulla [8].

During stress, these hormones induce various protective changes, which ultimately contribute to the restoration of body homeostasis. In particular, both glucocorticoids (GCs) and catecholamines (CAs) are known to acutely increase plasma glucose levels, promote elevated cardiac output, maintain high blood pressure, and to suppress inflammation [5].

#### **1.4 Steroid hormone synthesis**

Each layer of the adrenal cortex produces steroid hormones from the precursor cholesterol. However, the specific steroid hormone produced differs in each layer because of zonal-specific enzymes. Once cholesterol enters the cell, steroidogenic acute regulatory protein (StAR) regulates cholesterol transport from the outer mitochondrial membrane to the inner mitochondrial membrane [15].

In the inner mitochondrial membrane, the cholesterol can then be converted to pregnenolone via CYP11A1 (cholesterol desmolase, or cholesterol side-chain cleavage, P450<sub>scc</sub>). CYP11A1 catalyzes the rate-limiting step of steroid hormone production, and it is expressed in all three layers of the adrenal cortex. Of note, ACTH induces steroidogenesis in all 3 zones by stimulating this rate-limiting enzyme [12]. The downstream fate of pregnenolone will depend on the specific enzymes within that zone.

Since the zona glomerulosa does not have 17 alpha-hydroxylase, pregnenolone can only be converted into progesterone via 3-beta-dehydrogenase; 21-hydroxylase catalyzes conversion to 11-deoxycorticosterone; 11-beta-hydroxylase catalyzes conversion to corticosterone. Finally, aldosterone synthase, which is present only in the zona glomerulosa and is regulated by angiotensin II, converts corticosterone into aldosterone.

Aldosterone, corticosterone, and deoxycorticosterone all have mineralocorticoid activity with aldosterone being the predominant mineralocorticoid in humans.

In the zona fasciculata, 17-alpha-hydroxylase converts pregnenolone and progesterone, which were synthesized in the glomerulosa, into 17-hydroxypregnenolone and 17-hydroxyprogesterone, respectively; 3-beta-dehydrogenase converts 17-hydroxypregnenolone into 17-hydroxyprogesterone; 21-hydroxylase converts 17-hydroxyprogesterone to 11-deoxycortisol; and 11-beta-hydroxylase converts 11-deoxycortisol to cortisol, the predominant glucocorticoid.

In the zona reticularis, 17-hydroxypregnenolone and 17-hydroxyprogesterone can be converted into DHEA and androstenedione by 17,20 lyase (17 alpha-hydroxylase). Although DHEA is predominantly made, some of it can be converted into androstenedione by 3 $\beta$ -hydroxysteroid dehydrogenase in the zona reticularis [14, 16].

## **1.5 Adrenal gland tumors**

Adrenal tumors include benign and malignant adrenocortical tumors, named adrenocortical adenomas and carcinomas, respectively, and benign and malignant tumors of the adrenal medulla, named pheochromocytomas. Adrenal benign masses are often referred to as adrenal incidentaloma since they are serendipitously findings during imaging procedures performed for a different purpose [17].

Among tumors of the adrenal cortex there are: adrenocortical adenoma (ACA) and adrenocortical carcinoma (ACC).

- Adrenocortical adenomas (ACA) are benign tumors that are frequent incidentally found during diagnostic imaging procedure performed for indications other than an evaluation for adrenal disease [18]. They grow in their primary location without invading other sites in the body, they grow slowly and have distinct and relatively smooth borders with cells that



resemble quite closely in size and shape with the ones of the normal tissue. Most ACAs are hormonally inactive and clinically silent, but they can also be associated to hormone excess giving rise to symptoms related to the secreted hormone [19]. The prevalence of excess cortisol secretion among ACAs ranges from 10 to 40%. Cortisol-producing adenomas most often result in mild autonomous cortisol excess and in some rare cases in Cushing's syndrome. If in the former the effects of hypercortisolemia are less evident, the latter is characterized by typical features including striae rubrae, plethora, uncontrolled hypertension, diabetes, weight gain and loss of mineral bone density [17, 20, 21]

The frequency of aldosterone hypersecretion (known also as primary aldosteronism or Conn's syndrome) varies from 1% to 10% according to the different studies [22, 23]. It is characterized by hyperaldosteronism resulting in hypertension and PA has been reported to constitute 5-10% of hypertension [24].

- Adrenocortical carcinomas (ACC) are malignant tumors, as opposed to the benign tumors, have cells that grow uncontrollably and spread locally and/or to distant sites. Carcinoma cells are usually larger, the edges of growth more irregular, and the heterogeneity is much more pronounced compared to an adenoma. ACCs can still produce steroid hormones like ACAs, with cortisol being the more common [25]. Since ACC is the topic of this project, it will be treated in detail in the next paragraph.

## **2. Adrenocortical carcinoma (ACC)**

### **2.1 Epidemiology**

Adrenocortical carcinoma (ACC) is a rare aggressive neoplasm with poor prognosis. ACC has an annual incidence of 0.5 -2.0 patients per million people per year and a bimodal age distribution with a peak <5 years of age and a second peak during the fourth to fifth decades of adult life, but the tumor can appear at any age [25-27]

Interestingly, the incidence of pediatric ACC is 10–15 times higher in children in southern Brazil, which is related to an inherited germline p53 mutation [28, 29]. ACC is slightly more common in women than men with a ratio of 1.5:1 [25].

### **2.2 Clinical presentation**

ACC may present with autonomous adrenal hormone excess or with symptoms caused by an abdominal mass. An increasing number of cases are diagnosed as incidentalomas ( $\approx$  10–15%), however, the likelihood of an adrenal incidentaloma being an ACC is low [18, 30]. About 50–60% of patients with ACC have clinical hormone excess. Hypercortisolism (Cushing syndrome) or mixed Cushing and virilizing syndromes are observed in most of these patients. Pure androgen excess is less frequent while estrogen or mineralocorticoid excess is very rare [31-34]. Non-specific symptoms from an abdominal mass include abdominal discomfort (nausea, vomiting, abdominal fullness) or back pain. Classical malignancy-associated symptoms such as weight loss, night sweats, fatigue or fever are rarely present [25].

### **2.3 Pathogenesis and genetics**

ACC pathogenesis is heterogeneous and still incompletely understood. Most of the progress in understanding its pathogenesis and identifying genes involved in ACC comes from the study of (rare) familial diseases. Although most cases of ACC are sporadic with no identifiable risk factor it can be a part of hereditary tumor syndromes [25, 35], which are summarized in Table 1.

Table 1. Hereditary ACC syndromes.

| <b>Syndromes</b>                           | <b>Mutated genes</b>   | <b>References</b> |
|--|--|-------------------|
| Multiple endocrine neoplasia type 1 (MEN1) | MENIN gene on chromosome 11q13   | [36]              |
| Li–Fraumeni syndrome (LFS):                | TP53, located on 17p13   | [37].             |
| Lynch syndrome                             | MSH2, MSH6, PMS2, MLH1, and TACSD1/EPCAM (genes involved in DNA mismatch repair genes)   | [38]              |
| Beckwith–Wiedeman syndrome (BWS)           | Alterations of DNA methylation of the 11p15 locus, which harbors the coding regions for Insulin-growth-factor 2(IGF2), the cell cycle regulator CDKN1C, and the non-translated RNA, H19. | [39]              |
| Familial adenomatous polyposis coli (FAP)  | Inactivating germline mutation of the tumor suppressor gene adenomatous polyposis coli (APC) gene, which encodes for a downstream regulator of the Wnt/ $\beta$ -catenin pathway         | [40]              |
| Werner syndrome                            | Premature aging disease caused by the mutation in the WRN gene.  | [41]              |
| Neurofibromatosis type 1 (NF1)             | Mutation in the NF1 gene that encodes neurofibromin  | [42]              |

In terms of the occurrence of sporadic ACC, somatic genetic alterations leading to changes in p53 signaling, Wnt- $\beta$ -catenin signaling, IGF2 overexpression, are some of the most often cited reasons [43-45]. A study published in 2014 based on the molecular analysis of 122 ACCs identified nine pathogenic genetic alterations that were present in at least 5% of ACCs [46]. The most frequently altered pathway was the Wnt- $\beta$ -catenin pathway with 39% of the genetic defects affecting this pathway. Signaling by the Wnt family of glycolipoproteins is one of the fundamental mechanisms that direct cell proliferation and cell fate determination during embryonic development and in adult organs, with  $\beta$ -catenin being the key effector responsible for transduction of the signal to the nucleus

[47]. Inside this pathway, the most common genetic abnormalities identified in ACC are the activating mutations of the Catenin Beta 1 gene (CTNNB1), and deletions in the Zinc and Ring Finger 3 (ZNFR3) gene that lead to activation of the Wnt/ $\beta$ -catenin pathway in ACC [43-45]. Consequently, activation of the Wnt pathway induces cell proliferation and resistance to apoptosis. Furthermore, the somatic mutation of the CTNNB1 is an independent predictor of less favorable survival in ACC [48].

The p53-Rb pathway was the second most frequently affected pathway, with the alterations identified in 33% of ACCs [43]. P53 has central roles in mediating the cellular response to genotoxic stress (such as ionizing radiation, free radicals, hypoxia and metabolic challenge) and oncogene activation, and fulfills these roles by activating pathways involved in cell-cycle arrest and DNA-damage repair. These responses to cellular stress are postulated to give the cell the opportunity to respond to the stress and to repair accrued DNA damage. Failing this, and in circumstances of catastrophic genomic compromise, however, p53 induces apoptotic pathways to abrogate propagation of a corrupted genome. In addition to these roles, p53 is known to mediate angiogenesis, cellular senescence and has recently been recognized to participate in the inflammatory response and in suppressing invasiveness. Non-functioning P53 can result in malignancy [49].

The insulin-like growth factor (IGF) pathway is involved in the development and in the maintenance of different biological functions in normal adrenal glands [50]. The pathway consists of ligands (IGF-1 and IGF-2), receptors, binding proteins and binding protein proteases. IGF2 is highly overexpressed in majority of ACCs [51] It can be used in combination with proliferation marker Ki-67 with great accuracy to differentiate ACC from ACA IGF2 regulates the growth and apoptosis of cells and interact with insulin-like growth factor 1 receptor (IGF1R). The latter is also found to be overexpressed in ACC [52]. Activation of IGF-1R results in stimulation of downstream signaling pathways including the mitogen-activated protein kinase (MAPK) and phosphoinositol3-kinase (PI3-AKT) pathway, leading to increased cell proliferation and survival [53]. IGF2 overexpression by LOH is associated with poorer outcome in ACC [54].

Several other growth factors have also been shown to be overexpressed in ACC, including transforming growth factor-beta 1 and 2 (TGF $\beta$ -1 and 2) [33, 55], vascular endothelial growth factor (VEGF) [56, 57] [58]. It has also been hypothesized that some sporadic ACCs could be a multistep process with possible progression from a benign to a malignant adrenocortical tumor [59] [60].

## **2.4 General prognosis**

The prognosis of ACC is heterogeneous with a five-years overall survival rate ranging from 15% to 80% according to tumor stage based on the European Network for the Study of Adrenal Tumors (ENSAT) European Network for the Study of Adrenal Tumors (ENSAT) classification [61]. Other independent prognostic factors are the resection status [62], the mitotic index Ki67 [63] and cortisol excess [64]. Particularly, incomplete microscopic (R1) or macroscopic (R2) resection, high mitotic index (Ki67 >20%) and hypercortisolism are associated with worst prognosis. A recent multicenter ENSAT study proposed the use of a score (S-GRAS) based on the combination of clinical and histopathological parameters (including ENSAT stage, grading defined by KI67 index, resection status, age and symptoms due to steroid autonomous secretion or tumor mass) to improve prognostication in ACC patient [65].

## **2.5 Diagnosis**

The ACC working group of the ENSAT has proposed standards for diagnostic procedures [33]. It is of most importance that each step of the management strategy should be decided in the setting of a multidisciplinary team including different expertise (endocrinology, radiology, pathology, surgery, oncology), in expert centers. An adrenal biopsy is not recommended, because of the increased risk of (needle-tract seeding) metastases, in the diagnostic work-up of patients with suspected ACC, unless, of course, there is already evidence of metastatic disease that interferes with surgery and thus histopathologic diagnosis is required to optimize oncological management.

## **2.6 Treatment**

Surgery is the mainstay of therapy and represents the only treatment modality able to offer a chance of a cure. Unfortunately, in half of patients the disease is diagnosed at an advanced stage and most patients radically resected have a relapse within the first 2 years [25, 66]. Therefore, the use of adjuvant treatment after tumor resection is strongly recommended in patients with high risk of recurrence (ENSAT tumor stage III, or microscopic residual tumor, or Ki67>10%) [25]. Moreover, advanced ACC patients, not eligible for surgery, are referred to systemic antineoplastic therapies. For decades, mitotane has been the reference drug for ACC both in adjuvant and palliative setting [67, 68].

Mitotane is an adrenal-specific cytotoxic agent, that mediated by the inhibition of sterol-O-acyl transferase (SOAT1) [69] . Because of a direct suppression of steroid production in the adrenocortical cells [70], mitotane plays an important role in palliation of effects of hypercortisolism from hormonally active ACC. Evidence for use of mitotane as the only approved drug for advanced ACC is based on retrospective series of data as opposed to any prospective, randomized controlled trials [71, 72].

This compound is considered efficacious when serum levels reach the so-called therapeutic range (14–20 mg/L) [73], which is not usually attained before 2–3 months of therapy. The delayed efficacy of mitotane provides the main rationale for its association with chemotherapy. Chemotherapy in fact exerts a cytotoxic effect in the first months of treatment when mitotane levels are not in the therapeutic range [66].

Mitotane was also found to potentiate the cytotoxicity of certain chemotherapeutic drugs by interfering with the multidrug resistant gene 1 product P glycoprotein (Pgp), which is also expressed by ACCs [74, 75]. Moreover, although mitotane is metabolized and cleared primarily by the liver, one of its most profound and dynamic influences is accelerating CYP3A4 activity. Since most medications are metabolized or altered by hepatic CYP3A4, mitotane therefore could have a significant impact on drug metabolism and drug-drug interactions [76].

Since 1993, a multicenter phase II trial started in Italy with the aim of testing the activity of mitotane administered in association to EDP (Etoposide, Doxorubicin and Cisplatin) in advanced ACC patients. Preliminary data have been published in 1998 [77] and the final results in 2005 [78].

The first and largest randomized phase III study in advanced ACC established etoposide, doxorubicin, cisplatin plus mitotane (EDP-M) as the cytotoxic chemotherapy of the first choice in metastatic ACC [79]. Locoregional strategies including surgery or radiotherapy are also used in cases with a residual disease of approximately 10% of the initial volume [25, 72]. In the meantime, several other therapeutic approaches have been investigated i.e. gemcitabine-capecitabine [80-82] or streptozotocin [79] but a clinically meaningful breakthrough has not yet been achieved, so there has been a growing interest in targeted therapies for the treatment of ACC [71, 83]. Overall, the advanced disease remains a major therapeutic challenge in patients with ACC.

### **3. Possible therapeutic targets in ACC**

#### **3.1 Progesterone receptors and estrogen receptors**

Progesterone (Pg) receptors (PgRs) and estrogen (E) receptors (ERs) are expressed at different intensities in both normal and neoplastic adrenal cortex [84]; however, the pathophysiological relevance of the steroid receptor expression in the physiological regulation of adrenal cell proliferation is not yet fully understood. In particular, in adulthood, ER- $\beta$  is expressed in the glomerular and fasciculate area of the adrenal cortex, while at the prepubertal age, it is mainly located in the reticular area [85, 86]. The ER- $\alpha$  subtype appears to be poorly expressed. During neoplastic degeneration, there is an unpredictable rearrangement of the expression of these receptors and data concerning the expression of the ERs are controversial. Indeed, the lack of ER- $\alpha$  and an increase of the ER- $\beta$  in the ACC have been reported by immunohistochemical analysis [84], while a decrease of ER expression has been observed as the ACC progresses [87, 88]. Finally, other studies demonstrated low ER- $\beta$  levels and/or high levels of ER- $\alpha$  in numerous cases of ACC, leading to an increase in the ER- $\alpha$ /ER- $\beta$  ratio compared to healthy tissue [86]. In the NCI-H295R cells, ER- $\beta$  gene expression is higher compared to ER- $\alpha$ , and the selective estrogen receptor modulator (SERM) 4-OH-tamoxifen inhibits cell proliferation [89, 90].

The expression of ER subtypes varies in different tissues, although they are often co-expressed [91]. The traditional paradigm is that ER- $\alpha$  is oncogenic and increases cell survival, while ER- $\beta$  exerts an opposite role, being protective and pro-apoptotic. This clear distinction, however, cannot be applied for each tissue and cell expressing both ER subtypes; indeed, ER- $\alpha$  has a dominant role in tissues such as the uterus, mammary glands, pituitary, skeletal muscle, adipose, and bone; whereas, ER- $\beta$  has a major role in the ovary, prostate, lung, cardiovascular, and central nervous systems [91].

PgR expression was as well detected in ACC [84]. Our group demonstrated that Pg exerts a cytotoxic effect on ACC cells via activation of PgR with the involvement of both genomic and non-genomic pathways [92, 93].

In breast cancer cells, PgR is a transcriptional target of ER, and estrogen is a well-known to stimulator of PgR synthesis [94]. Similar results have been obtained in human endometrial carcinoma [95]. Interestingly, in a rare and peculiar setting such as pregnancy in ACC patients, in which there are elevated levels of both Pg and E hormones, their role in the control/progression of the disease is controversial. Indeed, a study in 12 pregnant ACC patients concluded that pregnancy is associated

with shorter survival and disease-free survival compared to control group [96], while another study on 17 treated ACC patients becoming pregnant during the follow-up, suggests that pregnancy seems to be not associated with worse clinical outcome [97]. However, as the authors correctly pointed out, pregnancy-associated ACC tended to be discovered at a more advanced stage. Thus, the possibility of a pregnancy-induced more rapid progression cannot be excluded, and the diagnostic and therapeutic delays probably account for the more severe presentation. Tamoxifen and medroxyprogesterone acetate combined treatment exhibited significant inhibitory growth effect on breast cancer [98], endometrial cancer [99], and cisplatin-resistant ovarian cancer cells [100]. This combination therapy appeared to be active in phase II studies enrolling endometrial carcinoma patients [101]. These data provided the rationale to explore the cytotoxic interaction between selective estrogen receptor modulators (SERMs), such as tamoxifen, and Pg in ACC.

### ***3.1.1 Role of progesterone as anti-tumoral drug***

Pg is a lipophilic hormone that plays a fundamental role in normal developmental and reproductive functions and disease processes [102]. Despite Pg being dysregulated in different types of cancer and associated with cancer progression in some tumors [103], several studies demonstrated its antitumoral effect by regulating various cancer cell phenotypes, including proliferation, apoptosis, angiogenesis and autophagy, in addition to migration and invasion [104]. Pg inhibits the proliferation of breast cancer and osteosarcoma cells [105], and contributes to the decreased progression of colorectal cancer [106-108], inhibiting cell proliferation [109]. Pg promotes apoptosis in endometrial cancer [110] and HeLa cells, arresting the progression from the G1 phase to the S phase [111]. Pg-induced autophagy was observed in astrocytes [112-114]. Moreover, increasing data suggest that Pg inhibits migration and invasion in breast [115], ovarian [116], and endometrial cancer cells, thereby reducing their invasive potential [117]. Despite the knowledge about the effect of Pg in ACC is still limited, data published in the last years by our group are in line with results demonstrating the role of this hormone as an anti-tumoral drug. Indeed, by investigating the therapeutic use of abiraterone acetate (AA) in preclinical models of ACC, our group demonstrated that its antiproliferative effect is due to the increased production of Pg. This hormone, through its receptors, was able to reduce cell viability in NCI-H295R cells and primary secreting ACC cultures, in a concentration-dependent manner [92, 93]. In addition, we showed that the reduction of  $\beta$ -catenin nuclear translocation may contribute to the Pg cytotoxic effect and that Pg combined with other drugs such as mitotane [92] or the CDK4/6 inhibitor ribociclib [118] enhances their antineoplastic activity.



### 3.2. WEE1

The WEE1 kinase family consists of three serine/threonine kinases sharing conserved molecular structures and encoded by the following genes:

1. WEE1 (WEE1 G2 Checkpoint Kinase),
2. PKMYT1 (membrane-associated tyrosine- and threonine-specific cdc2-inhibitory kinase),
3. WEE1B (WEE2 oocyte meiosis inhibiting kinase).

WEE1 and PKMYT1 act as tumor suppressors in non-malignant eukaryotic somatic cells. As part of the DNA damage response (DDR) pathways, their main biological function is to prevent replication of cells with altered DNA. Similarly, WEE2 regulates cell cycle progression and meiosis [119].

WEE1 is a serine-threonine kinase that arrests cell cycle at the G2 checkpoint through inhibitory phosphorylation on Tyr15 of the cyclin-dependent kinase 1 (CDK1) and preventing the entry into mitosis allowing DNA repair during DNA damage. [120]. WEE1 inhibition results in high CDK1 activity and cells progress without arresting at the G2/M checkpoint, leading to a not adequate DNA damage repairing, which generates mitotic catastrophe and cell death [121]. In addition to the checkpoint function at the G2/M border, recent findings highlighted a role of WEE1 in the regulation of replication dynamics during S phase (intra S phase checkpoint). When cells reach the S phase, replication origins, triggered through the activation of the pre-replication complex and following the activation of S phase specific CDK, primarily CDK2. Similarly, to CDK1, CDK2 regulation is controlled through Tyr15 phosphorylation status by WEE1 that slows cell cycle progression through the S phase, stabilizing replication forks and preventing DNA double-strand breaks, thus providing an opportunity for DNA damage repair [120, 122]. Inhibition of WEE1 leads to DNA double-stranded breaks [121].

WEE1 may be particularly important in p53-deficient cancers, such as ACC, where TP53 mutations occur in 67% of tumors [123, 124]. Indeed, loss-of-function mutations in TP53 leave cells completely dependent on the ATR-CHK1-WEE1 axis for G2/M checkpoint control and also prevent cell cycle arrest at the G1 checkpoint, allowing entry into the S phase prior to repair of damaged DNA [120].

Therefore, targeting WEE1 for inhibition and compromising the G2/M checkpoint together with the S phase presents an opportunity to potentiate DNA-damaging therapy.

### ***3.2.1 Therapeutic potential of adavosertib, a WEE1 inhibitor***

Adavosertib (AZD-1775) is a highly potent and selective WEE1 inhibitor, that induces S and/or G2/M cell cycle checkpoints override, depending on cancer types, when used in monotherapy. Cell cycle perturbation is associated with a progressive accumulation of DNA damages and by the induction of apoptosis [119, 125]. This last event is cell cycle phase-dependent and it can occur (i) as a consequence of S phase checkpoint override, when cancer cells start DNA replication even in the presence of DNA damages (replicative catastrophe); (ii) following G2/M phase checkpoint override, that results in forced entry into mitosis, even in the presence of DNA damages (mitotic catastrophe) [119, 126].

Single-agent adavosertib demonstrates high activity in recurrent uterine serous carcinoma, which has frequent TP53 mutations and increases replication stress.

In combination strategies, adavosertib enhances the cytotoxicity of chemo/radiotherapy agents, by inducing cell cycle checkpoint override, inhibition of DNA damage repair, and induction of apoptosis [125, 127]. A phase I dose escalation study of adavosertib in combination with gemcitabine, cisplatin, or carboplatin shows safety and efficacy with a numerical, but not significant, improvement in response rate among patients with advanced solid tumors with versus without TP53 mutations [120]. Three phase II studies of adavosertib with chemotherapy demonstrate encouraging antitumor efficacy in patients with TP53-mutated or TP53-unselected ovarian cancer, sensitive or refractory/resistant to platinum-based therapy [128-130], including significant improvements in PFS and OS as compared to chemotherapy alone [129]. Subsequent trials of adavosertib in combination with docetaxel and cisplatin, gemcitabine and radiation, or irinotecan show favorable clinical activity in patients with TP53-unselected locally advanced head/neck squamous cell carcinoma [122], pancreatic cancer [131], and relapsed refractory pediatric solid tumors [132], respectively.

### **3.3 FGF/ FGFR pathway**

The fibroblast growth factor (FGF)/ FGF receptor (FGFR) signaling system regulates fundamental developmental pathways of multiple organ systems and plays an important role in many physiological and pathological processes in the adult organism, including the regulation of angiogenesis, tissue homeostasis, wound repair and neoplastic transformation by modulating proliferation, differentiation, survival, migration and metabolism of the cells [133-135]. The FGF family contains 22 members, usually divided into seven subfamilies, according to their shared structural and functional features; 18 among these, called canonical FGFs, are paracrine/autocrine

proteins that bind and activate the tyrosine kinase (TK) receptors FGFRs. [136]. The FGFR family consists of four structurally related members: FGFR 1, 2, 3 and 4, comprised of an extracellular domain, a transmembrane domain, and a split cytoplasmic TK domain [137]. Alternative splicing of the IgIII extracellular fragment of FGFR1 to 3 may generate isoforms that differ in terms of ligand-binding specificity, with IgIIIb and IgIIIc specifically expressed predominantly in epithelial and mesenchymal cells, respectively. [138-140]. Interaction of FGF ligands with their signaling receptors is regulated by protein or proteoglycan cofactors and by extracellular binding proteins[141]. Activated FGFRs phosphorylate specific tyrosine residues that mediate interaction with cytosolic adaptor proteins and the RAS-MAPK, PI3K-AKT, PLC $\gamma$ , and STAT intracellular signaling pathways [139].

The pathways activated by the binding of FGFs to their receptors are critical for adrenal development and maintenance. The transcriptional coactivator CITED2, which is important for the development of the adrenal glands, is under control of basic FGF (bFGF, also known as FGF2) in adrenocortical cells [142]. FGF-1 and FGF-2 are expressed in the adrenal cortex and are the most powerful mitogens for adrenocortical cells. Looking at the receptors, FGFR1 and FGFR4 are the most strongly expressed in the adult adrenal cortex, while FGFR2 is required for proper adrenal morphology by regulating cell adhesion and junction dynamics through cadherin expression modulation [143]. Indeed, deletion of FGFR2, results in various degrees of adrenal hypoplasia after birth. [144]. No FGFR3 was detectable in the fetal adrenal, and FGFR1 mRNA was expressed at barely detectable levels [145]. In adult adrenals, steroidogenic cells appeared to express FGFR2 and FGFR3, whereas all four receptors were detectable in the microvasculature [146]. A complete review can be found in [147].

### ***3.3.1 FGFR dysregulation in cancer.***

There is compelling evidence that atypical regulation of the FGF/FGFR system occurs in human tumors due to various genetic alterations affecting different members of the FGF or FGFR families. Gene amplifications were the most identified aberrations, present in 66% of the samples, often reported in FGFR1 and FGFR4 with variable frequencies among the different cancer types; fusions were predominantly seen in FGFR2 and FGFR3 [148, 149]. When FGFRs are mutated or amplified, aberrant activation of downstream pathways results in mitogenic and antiapoptotic responses in cells. FGF ligands are also known to promote tumor growth and proliferation by inducing neo-angiogenesis [150], through indirectly synergizing VEGF and platelet-derived growth factor pathways [151]. Furthermore, preclinical studies demonstrated FGFR crosstalk with other cell surface receptors such as G-protein-coupled receptors or other receptor tyrosine kinases such as epidermal

growth factor receptor, opening doors for possible therapeutic interventions with combination therapies [152].

Analyses of mutations [45] and mRNA expression [153, 154] patterns in ACC have identified disturbances in FGFR cascade with a range of 0% (for FGFR1) to 6% (for FGFR4) of cases [83, 147]. Amplifications of FGFR1, FGF9, or FRS2 were discovered in 3 out of 28 (10.7%) tumors of patients with ENSAT tumor stage III-IV by comparative genomic hybridization [155]. Giordano et al. showed that FGFR1 is among the most differentially expressed genes in ACC [53]. Using genome-wide expression studies, FGFR4 overexpression has been observed in adult but particularly in pediatric adrenocortical tumors (ACT) [55, 156, 157]. However, the molecular mechanisms responsible for FGFR4 upregulation in ACTs have been assessed only later by Brito et al. [158]. The authors not only confirmed the previous observations by demonstrating FGFR4 overexpression in a significant proportion of pediatric (88%) and adult (47%) ACTs, but also detected FGFR4 amplifications in 13.5% of the pediatric and 30.4% of adult ACTs, suggesting that gene amplification could be the cause of FGFR4 overexpression, at least in a subset of tumors [158]. Moreover, in line with previous data [55], they found a positive correlation between FGFR4 and IGF2 expression levels, suggesting that FGFR4 and IGF2 belong to a cluster of genes that are simultaneously overexpressed in ACC.

Recently, the Würzburg group published the results of 93 FGF pathway related genes in a large cohort of benign and malignant adrenocortical tissues, non-adrenal tissues and cell lines. Among the 11 genes expressed at lower levels in ACC compared to adrenocortical adenomas (ACAs), there were FGF12, FGF14, and FGFR2. The five genes significantly upregulated in ACCs vs ACAs encoded for the FGFR1, FGFR4, FGF8, and FGF19. FGF21 was the only analyzed gene that was expressed at significantly higher levels in advanced ACC. The expression of FGFRs was confirmed in a larger cohort of FFPE tissues using RNA in situ hybridization and correlated with clinical data confirming that FGFR1 and 4 were overexpressed in ACC compared to ACA, while FGFR2 was higher expressed in ACA. Moreover, a higher expression of FGFR4 was found in late ENSAT stages compared to early-stage and in recurrences/metastases compared to primary tumors [159]. Both FGFR1 and FGFR4 overexpression were significantly associated with worst prognosis [158, 159].

Some authors hypothesized that also FGFR2 expression may play a role in ACC since it regulates the differentiation and the spatial organization of the adrenal gland and it has also been linked to the activation of the Wnt/beta-catenin pathway [160], a key mechanism of adrenocortical tumorigenesis [161]. A pilot study in 26 ACCs analyzed CTNNB1 mutation status and FGFR2 expression in the same samples. The most striking result was a subset of tumors with high nuclear FGFR2 expression. However, although most tumors with the higher nuclear FGFR2 expression did not harbour a CTNNB1 mutation, the authors did not find a statistically significant association

between FGFR2 expression and the mutational status of CTNNB1 or distinct clinical features with [162].

### ***3.3.2 Therapeutic potential of FGFR inhibitors***

FGFR inhibitors emerge more often as potential targeted therapeutic agents [163]. Particularly, preclinical studies suggest that patients presenting genomic alterations are more likely to be sensitive to FGFR inhibitors [164, 165]. Pemigatinib and infigratinib received approval by FDA for the treatment of advanced unresectable cholangiocarcinoma harboring FGFR2 fusions or rearrangement, and erdafitinib for treatment of metastatic urothelial carcinoma with FGFR2 and FGFR3 genetic aberrations [152]. The preliminary molecular results would support the use of selective FGFR inhibitors also for treatment of ACC but, as of yet, these kinases have not often been targeted in dedicated trials [166]. A phase II trial including 17 patients with unresectable ACC, investigated the efficacy of dovitinib, a multi-kinase inhibitor with nonselective activity against the FGFR (targeting also colony stimulating factor 1 receptor/CSF1R and VEGF) [167], reported only one partial response. However, 23% of patients achieved stable disease lasting longer than 6 months.

A phase 1/2 study (NCT01752920) of another pan-FGFR inhibitor, ARQ087, included one ACC patient with FGFR1 gene amplification who experienced disease stabilization for 3.5 years, with a maximum tumor reduction of 20% post treatment [168]. Notably, FGFR inhibitors elicit their antitumoral effects not only directly on the cancer cells, but also indirectly through paracrine signaling blockade. Moreover, the simultaneous inhibition of FGF and CSF1 or VEGF signaling should enhance the antitumoral effects through targeting also potential immune evasion and angiogenesis in the tumor microenvironment [169], suggesting that multi-pronged therapy strategies directed at several targets would probably improve the modest results obtained until now. Thus, FGFRs potentially offer novel therapeutic targets also for adrenocortical carcinoma, a type of cancer often resistant to conventional antimitotic agents [147].

## 4. Aim of the project

ACC is a rare malignant neoplasm with a dismal prognosis, in particular in advanced and metastatic disease. For patients with metastatic ACC, treatment includes mitotane, platinum-based chemotherapy (EDP-M) and locoregional strategies [25, 72]. However, the progression of advanced disease occurs almost invariably and there are no defined second and following lines of treatment [170], identifying this as an unmet need. Thus, the general aim of my project was to find new druggable therapeutic targets.

Based on previously goals achieved by two research groups that supported this thesis project, we focused our attention on the druggable role of the Pg/PgR and E/ER pathways as well as the WEE1 kinase and FGF/FGFR family.

The first part of this project aimed at exploring the possible role of PgR and ER as new potential ACC therapeutic targets, investigating whether they are expressed in ACC tissues and if they could mediate the cytotoxic interaction between selective ER modulator tamoxifen, and Pg in ACC cell models.

Then, the role of Pg and PgR molecular mechanisms underlying the cytotoxic effect was deeply studied, with a particular interest to evaluate whether Pg could influence ACC cell invasiveness and metastasis formation both in *in vitro* and *in vivo* models.

Another possible target studied was the WEE1, focusing the project to evaluate the expression of WEE1 in ACC tissues and to investigate the effect of WEE1-inhibitor adavosertib alone or in combination with cisplatin or gemcitabine *in vitro*, particularly in p53-mutated cancer cells, although not exclusively.

Finally, another potential targetable pathway in ACC was studied, namely, the FGF/FGFR pathways. This project is geared to assess the *in vitro* cytotoxic and antiproliferative effects of drugs inhibiting the FGF/FGFR pathway, since several studies have demonstrated that, in particular FGFR1 and FGFR4 are upregulated in malignant compared to benign adrenocortical tumours and that their high expression was significantly associated with worse patient prognosis, suggesting that they are potentially interesting therapeutic targets.

## **5. Materials and methods**

### **Cell Lines**

The human NCI-H295R cell line, derived from a primitive ACC in a female patient [171], was obtained from the American Type Culture Collection (ATCC) and cultured as indicated by ATCC. MUC-1 cell line, established from a neck metastasis of an EDP-M-treated male patient, was kindly given by Dr. Hantel and cultured as suggested [172]. CU-ACC1 and CU-ACC2 cell lines were obtained from Dr. Katja Kiseljak-Vassiliades [173]. JIL-2266 patient-derived cell line was established by group of Würzburg [174]. Additionally, the new ACC cell line TVBF-7 [175] was established from a primary culture (formerly ACC115m) derived from a perirenal lymph-node metastasis of a male ACC patient who underwent progression after EDP-M. A detailed description of these cell lines can be found in Sigala et al. [176]. All cell lines were periodically tested for mycoplasma and authenticated by genetic profiling using polymorphic short tandem repeat (STR) loci with the PowerPlex Fusion system (Promega, BMR Genomics Cell Profile service).

### **Cell Treatments**

#### **Part I: assessing the potential of estrogen, progesterone and their receptors in ACC**

Preliminary experiments of concentration–response curves were conducted in the ACC cell cultures to establish the optimal drug concentration range of treatment. Cells (20000 cells/well) were seeded in 24-wells-plates and treated with increasing concentrations of Pg (0.1–160  $\mu$ M; Merck) and tamoxifen (0.1–20  $\mu$ M; Selleckchem); both drugs were solubilized in DMSO. Cell viability was evaluated by 3-(4,5-Dimethyl-2-thiazol)-2,5-diphenyl-2H-tetrazolium bromide (MTT) dye reduction assay according to the manufacturer protocol (Merck).

All the subsequent sets of experiments were conducted treating the cells for 4 days using their respective Pg IC<sub>50</sub> values (H295R: 25  $\mu$ M; MUC-1: 67,58  $\mu$ M; TVBF-7: 51,56  $\mu$ M), unless otherwise specified. All experiments were conducted in charcoal-dextran-treated serum (CTS).

#### **Part II: Potential role of WEE1 inhibitor in ACC**

Cells (50000 cells/ well) were seeded in 96-wells black plates and treated for 4 days with increasing concentrations of adavosertib (0.1-100  $\mu$ M; Selleckchem), cisplatin (1- 100  $\mu$ M;

MedChemExpress) and gemcitabine (0.05 – 50  $\mu$ M; MedChemExpress). All drugs were solubilized in DMSO. Cell viability was evaluated by CellTiter-Glo® assay (Promega).

### **Part III: potential role of FGF/FGFR pathway in ACC**

Cells were treated for 4 days with increasing concentrations of erdafitinib (0.01 nM – 60  $\mu$ M; MedChemExpress), rogaratinib (1 nM -100  $\mu$ M; Bayer) and fisogatinib (BLU-554) (1 – 200  $\mu$ M; Selleckchem). All drugs were solubilized in DMSO. Cell viability was evaluated by CellTiter-Glo® assay (Promega).

### **Drug Combination Experiments**

Combination experiments were performed according to the Chou and Talalay method [177]. Cells were treated for 4 days using increasing concentrations of each drug as single drug and in combination, as recommended for the most efficient data analysis. The drug concentration curve for the combination has been designed for each ACC cell model based on the respective IC<sub>50</sub> of each drug. Data were then converted to Fraction affected (Fa, range from 0 to 1 where Fa = 0 indicating 100% cell viability and Fa = 1 indicating 0% cell viability) and analyzed using the CompuSyn software (ComboSyninc) to calculate the Combination Index (CI). A CI value <1, = 1, and >1 indicates synergism, additive effect, and antagonism respectively.

### **Measurement of cell apoptosis**

Pacific Blue™ Annexin V/ SYOX™ AADVanced™ apoptosis kit (Invitrogen) was used to investigate Pg-induced cell death. ACC cells (5 x 10<sup>5</sup> cells/well) were seeded in a 6-well plate in a complete medium, 24hours(h) later cells were treated for 24, 48, 72, or 96h using their Pg IC<sub>50</sub> values. Cells were collected, washed with ice-cold PBS, resuspended in the binding buffer, and stained with Pacific Blue™ Annexin V/SYOX™ AADVanced™, according to the manufacturer's instructions. Cells were then analyzed using a MACSQuant10 cytometer (Miltenyi), using unlabeled cells as a negative control. Quantification of apoptosis was determined by FlowJo v10.6.2 software. Annexin V+/SYTOX- and Annexin V+/SYTOX+ cells were considered as early and late phase apoptotic cells, according to the manufacturer's instructions.

### **Cell cycle analysis**

For flow cytometric cell cycle analysis, untreated and Pg-treated cells were fixed, treated with Rnase A (12.5  $\mu$ g/mL) (Thermo Fisher Scientific), stained with propidium iodide (40  $\mu$ g/mL)



(Invitrogen), and analyzed by flow cytometry using a MACS Quant Analyzer (Miltenyi Biotec GmbH) for cell cycle status. Data were analyzed using FlowJo software (TreeStar).

### **Drug withdrawal experiments**

ACC cells were plated in 24-well plates and treated with their  $IC_{50}$  value of Pg for 4 days. At the end of the treatment, the drug-containing medium was replaced by a fresh complete medium without the drug and cell viability was evaluated at different times, up to 10 days (about twice the doubling time). Cells were analyzed for cell viability by 3-(4,5-Dimethyl-2-thiazol)-2,5-diphenyl-2H-tetrazolium bromide (MTT) dye reduction assay according to the manufacturer protocol (Merck).

### **Fish and embryos maintenance**

Zebrafish were maintained and used according to EU Directive 2010/63/EU for animal use following protocols approved by the local committee (OPBA) and authorized by the Ministry of Health (Authorization Number 393/2017). Adult transgenic line Tg (kdr1:EGFP) zebrafish lines were maintained at 28 °C in 14 h light and 10 h dark cycle in a circulating system maintained at pH 7.0–7.5, and conductivity between 400–500  $\mu$ s. Fish were fed with a combination of granular food (Special Diet Services, SDS, Witham, UK) and freshly prepared Artemia sp. (SDS, Witham, UK). Breeding of adult male and female zebrafish was carried out by natural crosses, and embryos were collected and raised in fish water (0.1 g/L Instant Ocean Sea Salts, 0.1 g/L Sodium Bicarbonate, 0.19 g/L Calcium Sulfate) with incubation at 28.5 °C until the experiments. The staging of zebrafish embryos was done according to established protocols. Embryos at 24 h post-fertilization (hpf) were treated with 0.003% 1-phenyl-2-thiourea (PTU) to prevent pigmentation. After the conclusion of the experiments, the zebrafish embryos were euthanized with 400 mg/L tricaine (ethyl 3-aminobenzoate methanesulfonate salt; Sigma-Aldrich, Milan, Italy)

### **Tumor xenograft**

To evaluate the toxic effect of Pg on the zebrafish model, 48 hpf wild-type embryos (AB) were divided into different groups as indicated and maintained in PTU/fish water to which solvent (DMSO) or increasing concentrations of Pg (10, 25, 50, and 100  $\mu$ M) were added. After 3 days (T3), effects of Pg were observed. To evaluate the effect of Pg on tumor growth, Tg (kdr1:EGFP) zebrafish embryos at 48 hpf were dechorionated, anesthetized with 0.042 mg/mL tricaine, and microinjected with the labeled tumor NCI-H295R, MUC-1, and TVBF-7 cells (CellTracker<sup>TM</sup> CM-Dil Dye, Thermo Fisher Scientific) into the subepidermal space of the yolk sac. Microinjections were

performed with a FemtoJet electronic microinjector coupled with an InjectMan N12 manipulator (Eppendorf Italia, Milan, Italy). Approximately 250 cells/4 nL were injected into each embryo (about 25 embryos/group); embryos were maintained in PTU/fish water in a 32°C incubator to allow tumor cell growth. Pictures of injected embryos were acquired using Zeiss Axiozoom V13 (Zeiss, Jena, Germany) fluorescence microscope, equipped with Zen pro software, 2h after cell injection (T0). 6.25, 12.5  $\mu$ M Pg or solvent (DMSO) were directly added to the PTU/fish water in respectively Pg-treated and untreated experimental groups. After 3 days (T3), the effects of the drug on cancer growth were scored taking pictures, as previously described, to measure the tumor areas of each group at T0 and T3 using Zen 2.3 Black software from ZEISS. Embryos with metastases (that is the presence of at least one fluorescence dot outside the site of injection) were counted and some representative xenografted embryos were fixed, embedded in low melting agarose, and acquired with LSM 510 confocal laser microscope equipped with Achropla 10x/0.25 objective.

### **Immunohistochemistry Part I**

Tissue samples were obtained from formalin fixed paraffin embedded (FFPE) tissues from surgical samples. The local Ethical Committee approved the project and written informed consent was obtained from the patients. 2  $\mu$ m thick sections were used for routine Hematoxylin and Eosin (H&E) staining and immunohistochemistry using the automatic stainer BenchMark ULTRA IHC/ISH System (Ventana). Diagnosis of ACC was revised according to the most recent WHO criteria [178]. The clinical characteristics of the patient are reported in Table 2. The following primary antibodies were used: anti-PgR clone 1E2, anti-ER clone SP1. All the primary antibodies were from “ready to use” kits from Ventana. Antigen retrieval was performed by incubation for 64 min for PgR and ER at 95°C in Ultra Cell Conditioning Solution (Ultra CC1, Ventana). Signal was revealed using the ultraView Universal DAB Detection kit (Ventana) followed by diaminobenzidine as chromogen and Hematoxylin for nuclear counterstain. Digital images were acquired by an Olympus XC50 camera mounted on a BX51 microscope (Olympus) using CellF Imaging software (Soft Imaging System GmbH). Expression of PgR and ER was semi-quantitatively scored on representative tumor areas based on both percentage: score ranges: 0 (0–5%), 1 (6–29%), 2 (30–69%), 3 ( $\geq$ 70%) and intensity (score ranges: 0, no expression; 1, weak; 2, moderate; 3, high) of immunoreactive (IR) neoplastic cells.

**Table 2: Clinical and immunohistochemical characteristics of ACC patients of Part I.**

| Code                                | Tumor specimen        | Histology                           | Disease stage | Hormone hypersecretion | SF-1 expression |
|-------------------------------------|-----------------------|-------------------------------------|---------------|------------------------|-----------------|
| <b>ACC29</b><br>Female<br>51 yr old | Primary ACC           | Mitotic index: 2/50 HPF; Ki67: <5%  | Stage IV      | Cortisol               | +               |
| <b>ACC32</b><br>Male<br>66 yr old   | Primary ACC           | Mitotic index: >5/50 HPF; Ki67: 20% | Stage II      | No secretion           | +               |
| <b>ACC55</b><br>Male<br>57 yr old   | Peritoneal metastasis | Ki-67 not homogenous: 8-10% 15-20%  | Stage IV      | No secretion           | +               |
| <b>ACC91</b><br>Female<br>62 yr old | Abdominal metastasis  | Ki-67 20%                           | Stage IV      | No secretion           | +               |
| <b>ACC115</b><br>Male<br>57 yr old  | Linfonodal metastasis | Mitotic index: 58x10HPF; Ki67: 22%  | Stage IV      | No secretion           | +               |

**Immunohistochemistry Part II**

For the WEE1 immunohistochemistry, FFPE tissue samples of 114 ACC with known *TP53* mutation status were analyzed. All tissues were collected between January 2005 and December 2017 at the University Hospital of Würzburg. The last follow-up was September 2022. All patients gave informed consent, and the study was approved by the ethical committee of the University of Würzburg (88/11). Clinical parameters, including sex, age at diagnosis, tumor type, hormone secretion, ENSAT tumor stage at diagnosis, Weiss score, Ki67 index, and clinical outcome were collected through the ENSAT Registry ([www.ensat.org](http://www.ensat.org)). Clinicopathological parameters are summarized in Table 3. For the evaluation of the *TP53* status, DNA was isolated from tumors with the GeneRead DNA FFPE Kit (Qiagen, Hilden, Germany) and from peripheral blood with the NucleoSpin Blood L Kit (Macherey-Nagel, Bethlehem, PA), as previously reported [179]. Tumor and leukocyte DNAs were enriched with the GeneRead DNaseq Human Comprehensive Cancer Panel V2 and GeneRead DNaseq Panel PCR Kit V2 (both Qiagen) including 160 genes, among which *TP53* gene. Molecular analysis of part of this cohort was already published by the group of Würzburg [179].

The immunohistochemistry procedure was performed as previously reported [180]. Briefly, full tissue sections were deparaffinized and rehydrated in descending graded of ethanol. Antigen retrieval was achieved in 10 mM citric acid monohydrate buffer (pH 6.5) in high temperature. Unspecific binding was blocked by 20% human AB serum in PBS. The primary antibody used was anti-WEE1 (#13084, Cell Signaling Technology, 1:1000). For the negative control the N-Universal Negative Control Anti-Rabbit (IS600, Dako, Glostrup, Denmark) was used. Signal amplification was detected by HiDef Detection HRP Polymer System (954D-50, Medac Diagnostika,) and DAB substrate kit (957D-30, Cell Marque). Nuclei were counterstained with Mayer's hematoxylin for 2 min (T865.1, Carl Roth). Images were acquired using the Leica Aperio Versa Brightfield scanning microscope (Leica) and evaluation of nuclear staining was performed by automated image analysis (Aperio ImageScope software).

**Table 3. Clinicopathological characteristics of the investigated ACC patients of Part II.**

|                                 | <b>RT-qPCR cohort</b> | <b>IHC cohort</b> |
|---------------------------------|-----------------------|-------------------|
| N of patients                   | 52                    | 113               |
| N of samples                    | 52                    | 114               |
| Sex (F:M)                       | 30:22                 | 67:46             |
| Age years                       | 50.5 (18-80)          | 50.5 (18-78)      |
| Tumor type:                     | 41 (78.9%)            | 96 (84.2%)        |
| Primary                         | 5 (9.6%)              | 12 (10.5%)        |
| Local recurrence                | 6 (11.5%)             | 6 (5.3%)          |
| Metastasis                      |                       |                   |
| Hormone secretion:              | 30 (57.7%)            | 43 (37.7%)        |
| Glucocorticoid (alone or mixed) | 9 (17.3%)             | 11 (9.6%)         |
| Androgens or aldosterone        | 8 (15.4%)             | 24 (21.1%)        |
| Inactive                        | 5 (9.6%)              | 36 (31.6%)        |
| Unknown                         |                       |                   |
| ENSAT tumor stage:              | 19 (36.5%)            | 56 (49.1%)        |
| I-II                            | 12 (23.1%)            | 30 (26.3%)        |
| III                             | 21 (40.4%)            | 28 (24.6%)        |
| IV                              |                       |                   |
| Resection status:               | 28 (53.9%)            | 87 (76.3%)        |
| R0-RX                           | 18 (34.6%)            | 23 (20.2%)        |
| R1-R2                           | 6 (11.5%)             | 4 (3.5%)          |
| unknown                         |                       |                   |
| Weiss score                     | 6 (3-9)               | 6 (3-9)           |
| Ki67% index                     | 20 (2-90)             | 15 (2-90)         |

### **Immunofluorescence**

Cells were grown onto 12 mm poly-L-lysine coated coverslips for 4 days and were then fixed with paraformaldehyde 4% (w/v) (Immunofix, Bio-Optica) for 15 min at 4°C and permeabilized with 20% MetOH and 0.1% Triton X-100 in PBS for 10 min. Non-specific binding was blocked by incubation in PBS containing 0.1% Triton X-100 and 0.2% of BSA for 45 min. Cells were incubated with anti-PgR (raised in rabbit, 1:800, Cell Signaling Technology), anti-ER- $\beta$  (raised in rabbit, 1:500, Abcam) and anti-ER- $\alpha$  (raised in mouse, 1:500, Invitrogen) primary antibodies o/n at 4°C. After extensive washes, the anti-rabbit Alexa Fluor 488 (green signal) and anti-mouse Alexa Fluor 555 (red

signal) (Immunological Sciences) secondary antibodies, and Alexa Fluor 647 Phalloidin (Invitrogen) were applied for 1 h at rt. After rinsing in PBS, coverslips were mounted using DAPI-containing Vectashield mounting medium (Vector Laboratories). Slides were observed by a LSM 880 Zeiss confocal laser microscope equipped with Plan-Apochromat 63×/1.4 numerical aperture oil objective or by a LSM 510 Zeiss confocal laser microscope (Carl Zeiss AG) equipped with Plan-Apochromat 63×/1.4 numerical aperture oil objective. Images were then reconstructed using Zeiss ZEN 2.3 Imaging Software (Carl Zeiss). The specific mean fluorescence intensity of the pixels was quantified using ZEN Black software (Carl Zeiss) and/or ImageJ software. Several fields, randomly chosen, were acquired and analyzed for each experimental condition.

### **Migration and invasion assay**

The motility and invasive capability of untreated and Pg-treated ACC cells were explored using the Transwell assays. For migration assay, QCMTM Chemotaxis 24-Well Cell Migration Assay with an 8 µm pore size (Merk) was used. The in vitro invasiveness of cells was evaluated using ECMatrix Cell Invasion Assay with an 8 µm pore size (Merck).

Cells were seeded in culture dish at an appropriate cell density. After 24 hours, cells were exposed to their respective IC50 value of Pg or vehicled in fresh medium for 96 h of treatment. Then, cells were detached using trypsin/EDTA, resuspended and added into the upper chamber of migration or invasion inserts according to manufacturers' protocols. The chemo-attractant gradient was created using a medium enriched with 10% of fetal bovine serum. After incubation in a humidified tissue culture incubator for 22h (for migration assay) or 72h (for invasion assay), the cells in the interior of the chamber that did not penetrate the membrane have been cleaned up. Penetrated cells were stained and after washing, inserts were air-dried. Images were acquired using an Olympus IX51 optical microscope (Olympus Italia, Segrate, Italy) equipped with a 10x objective. Subsequently, staining was eluted, and absorbance was detected using an EnSight Multimode Plate Reader (PerkinElmer) at 560nm.

### **Wound healing assay**

To evaluate the wound healing assay, cells were cultured in a 6 wells plate until reaching 90%–100% confluency at which point a scratch was created using a p200 pipette tip. Media was removed and cells were washed in PBS before adding the medium conditioned with vehicle or Pg. Five different areas along the scratches of each well were analyzed by optical microscopy after 0 and 24h following the induced damage. The distance between each edge of the scratch was monitored under an Olympus IX51 microscope and was measured using the software NIH ImageJ Software.

## **Western blot**

Cells were homogenized in cold RIPA buffer, and total protein concentrations were determined by Bio-Rad Protein Assay (Bio-Rad Laboratories). Equal amounts of proteins (30 µg) were run in 10% polyacrylamide gels and transferred onto a polyvinylidene fluoride (PVDF) membrane. Anti-LC3 primary antibody (Sigma) and secondary HRP-labeled anti-rabbit antibody (Promega) were used. Densitometric analysis of the bands was performed by using NIH ImageJ Software. To evaluate secreted MMP2 levels, the conditioned medium was obtained as described [181]. Briefly, equal amounts of untreated and Pg-treated cells were seeds in a free-serum medium (1x 10<sup>6</sup> cells/ 1 ml medium). After 2h, conditioned media were collected, stored at -80°C for at least 24h, and subsequently freeze-dried. The residues were resuspended in the same volume of PBS. Next, proteins were separated by electrophoresis on a 4–12% NuPAGEbis-tris gel system (Life Technologies, Italy), electroblotted to a PVDF membrane, and finally detected using an anti-MMP2 primary antibody (Proteintech).

## **Zymography**

Novex 10% Zymogram Plus (Gelatin) gels (Thermo Fisher Scientific) were used to measure secreted MMP2 activity in conditioned media. Different aliquots of the same conditioned medium samples were used for both western blot and zymography. The proteins were separated by electrophoresis on a 4-12% sodium dodecyl sulfate (SDS)-PAGE gel run under denaturing conditions. and visualized as clear bands against a dark background using a renaturing, developing, and staining protocol (Thermo Fisher Scientific).

## **Gene expression Part I**

Preliminary experiments to evaluate the gene expression of different metalloproteases (MMPs) in NCI-H295R, MUC-1 and TVBF-7 cell lines were performed using the Human Tumor Metastasis RT2 Profiler PCR Array (Qiagen). The RNA isolation, the treatment with DNase, and the RNA purification were performed using the Qiagen kit (Qiagen). For cDNA synthesis, the RT2 First Strand Kit (Qiagen) was used. The PCR was performed with ViiA7 (Applied Biosystems) using RT2 SYBR Green qPCR Mastermix (Qiagen) as fluorochrome.

For the other gene expression analysis total RNA was extracted from cells using the RNeasy kit (Qiagen) and 1 µg was transcribed into cDNA, using murine leukemia virus reverse transcriptase (Promega). Gene expression was evaluated by q-RT-PCR (ViiA7, Applied Biosystems) using SYBR

Green as fluorochrome. Sequences of oligonucleotide primers were reported in Table 4. Expression levels were normalized to the  $\beta$ -actin mRNA level of each sample, obtained from parallel assays.

Table 4. Sequences of gene oligonucleotide primers for qRT-PCR

| Gene           |        | Oligonucleotide Sequence (5'-3')                |
|----------------|--------|---|
| $\beta$ -ACTIN | F<br>R | TCTTCCAGCCTTCCTTCCTG<br>CAATGCCAGGGTACATGGTG    |
| ER- $\alpha$   | F<br>R | CCACCAACCAGTGCACCATT<br>GGTCTTTTCGTATCCCACCTTTC |
| ER- $\beta$    | F<br>R | AGAGTCCCTGGTGTGAAGCAAG<br>GACAGCGCAGAAGTGAGCATC |
| PgR            | F<br>R | CGCGCTCTACCCTGCACTC<br>TGAATCCGGCCTCAGGTAGTT    |
| SF-1           | F<br>R | CAGCCTGGATTTGAAGTTCC<br>TTCGATGAGCAGGTTGTTGC    |
| MMP-2          | F<br>R | ACGACCGCGACAAGAAGTAT<br>ATTTGTTGCCAGGAAAGTG     |
| TIMP1          | F<br>R | GGGACACCAGAAGTCAACCA<br>GGCTTGGAACCCTTTATACATC  |
| TIMP2          | F<br>R | AAGCGGTCAGTGAGAAGGAA<br>TCTCAGGCCCTTTGAACATC    |

### Gene expression Part II and III

RNA was isolated with the Maxwell RSC Simply RNA Kit (Promega) from fresh frozen tissues and five cell lines for the evaluation of *WEE1* expression and from six cell lines for the evaluation of different *FGF* receptors.

RNA concentration was determined using a Nanodrop Spectrophotometer (Thermo Fisher) and 1000 ng RNA were reverse transcribed with the QuantiTect RT Kit (Qiagen). Quantitative reverse transcriptase PCR (RT-qPCR) was performed using TaqMan gene expression probes (Thermo Fisher Scientific) for *WEE1* (Hs00268721), *FGFR1 IIIb* (Hs659A1), *FGFR1 IIIc* (Hs659A2), *FGFR2 IIIb* (Hs659A3), *FGFR IIIc* (Hs659A4), *FGFR4* (Hs01106908). Endogenously expressed *ACTB* (Hs99999903) was used as housekeeping gene for normalization. For each RT-qPCR reaction, 5 ng cDNA were used, and each sample was analyzed in technical duplicates. All transcripts were amplified using TaqMan Gene Expression Master Mix (Thermo Fisher) using the CFX96 real-time



thermocycler (Bio-rad) and the Bio-rad CFX Manager 2.0 software. Cycling conditions were 95°C for 3 min, followed by 39 cycles of 95°C for 30 s, 60°C for 30 s and 72°C for 30 s. Fold change was calculated using the  $\Delta$ CT method, normalized to housekeeping gene  $\beta$ -actin.

Particularly, for the *WEE1* evaluation, 90 adrenocortical snap-frozen tissues, including 19 normal adrenal glands, 20 ACAs and 52 ACCs, were included. As for the FFPE samples, all patients gave informed consent (Ethical committee of the University of Würzburg 88/11). Clinicopathological parameters of this cohort of ACC patients are summarized in Table 3.

### **Statistical analyses**

Statistical analysis was carried out using GraphPad Prism (version 5.02, GraphPad Software) and SPSS Software (PASW Version 28.0). Continuous variable evaluated by non-parametric test. One-way ANOVA with Bonferroni's correction was used for multiple comparisons. Unless otherwise specified, for cell experiments, data are expressed as mean  $\pm$  Standard Error of mean (S.E.M.) of at least three experiments run in triplicate. For the *WEE1* part, clinical and pathological parameters were correlated with *WEE1* expression both as mRNA and protein levels. For the clinical outcome, overall survival (OS) and progression-free survival (PFS) were considered. OS was defined as the time from the primary surgery to disease-related death or last follow-up and was evaluated only in primary tumor tissues. PFS was defined as the time from the surgery or diagnosis (in case of ENSAT stage tumor) to the first radiological evidence of disease progression or disease-related death. Survival curves were obtained by Kaplan-Meier and log-rank (Mantel-Cox) test. Multivariate regression analyses were performed by Cox proportional hazard regression. P values  $< 0.05$  were considered statistically significant.

## 6. Results

### 6.1 Results Part I: assessing the potential of estrogen, progesterone and their receptors in ACC

#### Estrogens in the ACC cell models

Due to the suggested different roles of ER in cell viability, we evaluated whether the ER- $\alpha$  and ER- $\beta$  subtypes were differentially expressed in ACC experimental cell models. ACC cell lines and the ACC115m primary cell culture were then investigated for ER gene and protein subtype expression. Results on gene expression are reported in Table 4, while the mRNA translation into the respective protein was demonstrated by immunofluorescence [90]. Concerning the ACC cell lines, NCI-H295R cells expressed both ER subtypes, although the gene and the protein both indicated a low level of expression with a prevalence of ER- $\beta$  over the ER- $\alpha$  [90]. Metastasis-derived MUC-1 cell line and ACC115m primary culture, displayed a very weak expression of ER- $\alpha$  and ER- $\beta$ , both at gene (Table 5) and protein levels [90]. We would like to underline the peculiar sub-cellular localization of the ER subtypes, as we can observe a prevalent nuclear localization of ER- $\beta$ .

**Table 5. ER gene expression in ACC cell lines and primary cell culture.**

| Target gene  | NCI-H295R        | MUC-1  | ACC115m          |
|--------------|------------------|--------|------------------|
| ER- $\alpha$ | 10.88 $\pm$ 0.36 | >15.00 | 11.50 $\pm$ 0.83 |
| ER- $\beta$  | 9.81 $\pm$ 0.38  | >15.00 | 13.43 $\pm$ 0.68 |

*Values were reported as  $\Delta Ct$  that are differences of the threshold cycle (Ct) values between the  $\beta$ -actin housekeeping gene and the gene of interest ( $\Delta Ct$ ), calculated, as described in Materials and Methods.*

To explore the possible involvement of ERs in ACC cytotoxicity and cell proliferation rate, ACC cell-lines were treated with increasing concentrations of tamoxifen for 4 days and then evaluated for cell viability. The ACC cell line NCI-H295R displayed a concentration-dependent cytotoxicity, with the IC<sub>50</sub> of 5.43  $\mu$ M (95% CI: 5.18–5.69  $\mu$ M) and the reduction of the cell proliferation rate. MUC-1 cell line and ACC115m primary culture were resistant to tamoxifen, in agreement with the very low ER expression in these ACC cell models. In particular, tamoxifen exposure did not show

any effect on cell viability up to 15  $\mu\text{M}$  and then a sharp decrease at 17.5  $\mu\text{M}$  and 20  $\mu\text{M}$ , more evident in ACC115m [90]. Whether this effect is ER-dependent or not needs to be determined.

### Pg in the ACC Cell Models

We already demonstrate that NCI-H295R cells express PgR (31) and that Pg exerts a concentration-dependent cytotoxic effect on NCI-H295R cells line as well as in ACC primary cell cultures expressing PgR [92]. Here, we confirmed this result in other ACC cell models, studying the Pg effect in metastasis-derived cell models, namely MUC-1 cell line and in ACC115m primary cells. We firstly assessed the PgR expression in these cells by q-RT-PCR. The  $\Delta\text{Ct}$  obtained was MUC-1:  $12.71 \pm 0.62$ ; ACC115m:  $10.39 \pm 0.04$  (cDNA belonging from NCI-H295R cells was used as internal positive control:  $\Delta\text{Ct}$ :  $9.48 \pm 0.57$ ), thus suggesting that PgR gene expression was present. Although a direct relationship between mRNA and proteins cannot be established, a correlation between the gene expression and the immunofluorescent signal in these ACC cell models could be observed. Indeed, PgR signal in MUC-1 cells and ACC115m primary cell culture is weaker compared to NCI-H295R cells [90]. A modest cytotoxic effect of both ACC cell models derived from metastatic patients was observed when cells were exposed to increasing Pg concentrations, suggesting that these cells were less sensitive to Pg compared to NCI-H295R cells. Indeed, the  $\text{IC}_{50}$  was 67.58  $\mu\text{M}$  (95% CI: 63.22–73.04  $\mu\text{M}$ ) for MUC-1 cells and 51.76  $\mu\text{M}$  (95% CI: 46.45–57.67  $\mu\text{M}$ ) for ACC115m cells (Figure 2A). Pg treatment affected the cell proliferation rate as well on each ACC cell model as reported in Figure 2B.

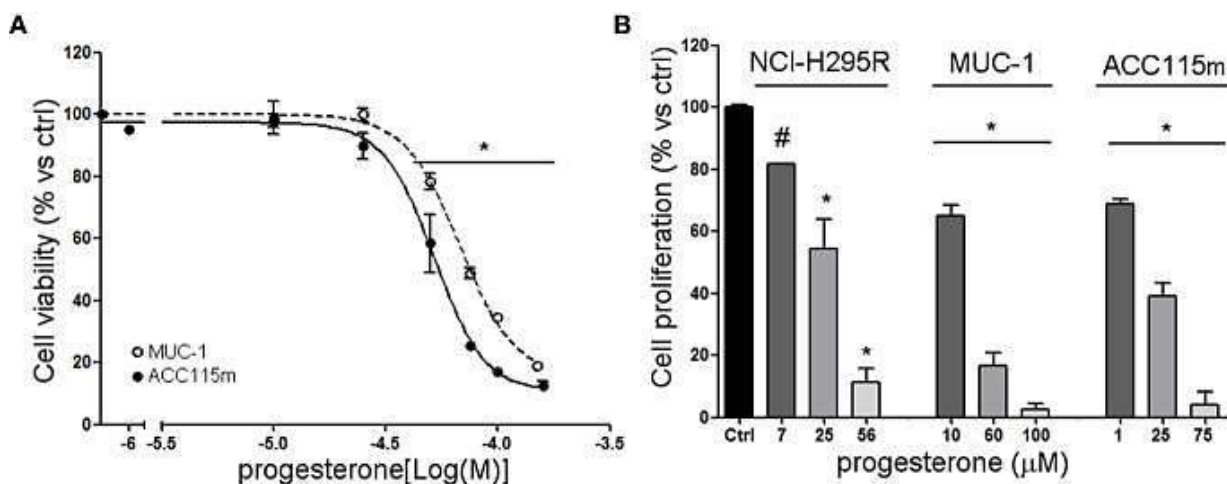


Figure 2. Cytotoxic effect of Pg in ACC cell models. (A) MUC-1 cell line and ACC115m primary culture were treated with increasing concentrations of progesterone (0.1–160  $\mu\text{M}$ ), then cell viability was analyzed by MTT assay, (B) NCI-H295R, MUC-1 cell lines and ACC115m primary culture were treated with low, intermediate, and high dose of Pg, and cell proliferation was analyzed by directing counting with trypan blue discrimination. Results are expressed as percent of viable cells vs ctrl  $\pm$  SEM; \* $P < 0.0001$  vs untreated cells; # $P < 0.01$  vs untreated cells.

### **Effect of drug combination treatment on ACC cell viability**

Due to the sensitivity of NCI-H295R cell line to both Pg and tamoxifen, we thus evaluated whether the cytotoxic effect of tamoxifen on NCI-H295R cell viability could be enhanced by Pg, applying the Chou–Talalay method for drug combination experiments [177]. Cells were exposed to increasing concentrations of tamoxifen (1.2–13.5  $\mu\text{M}$ ) and Pg (7.4–84.3  $\mu\text{M}$ ) at 1:6.17 fixed molar ratio for 4 days and then analyzed for cell viability by MTT assay. The combination index was then calculated, and the analysis revealed a prevalent antagonist effect when the two drugs were combined. Finally, since mitotane is the standard treatment for ACC patients, we then evaluated the combined treatment NCI-H295R cell line as well with tamoxifen and mitotane. Results showed that the combination has an additive/synergic effect at low concentrations, while, as the drug concentrations increased, the antagonism prevailed [90].

### **PgR and ER expression in ACC tissues**

Finally, the expression of ER and PgR was studied by immunohistochemistry in 36 paraffin embedded tumor samples belonging to ACC diagnosed patients. Among this cohort, 13 patients were male and 22 females, with an age median of 53 years (range: 16–79 years), 11 of them were cortisol-secreting, while the others were not secreting. Results reported in Table 6 indicated that ERs were absent or present with a very weak expression, while PgR were expressed, although with variability between the different samples. In particular, concerning the ER positive cells, we could observe that only three ACC samples displayed a percentage of ER moderately positive cells within the range of 30–69%, while 28 of the ACC samples had less than 5% ER positive cells, with a null to low intensity. Concerning PgR, there was evaluable expression in each sample studied, with only three ACC samples having less than 5% of PgR immunoreactive cells. Indeed, almost half of samples contained between 30 and 69% of immune positive cells and eight samples up to 36 expressed more than 70% of positive cells. A representative example of immunohistochemistry conducted on some ACC tissues is reported in [90]. The clinical characteristics are reported in Table 2.

In detail, ACC29 cells showed a tumor with lobulated morphology, moderate atypia and few mitotic figures. This tumor exhibits focal and moderate PgR expression, scant ER IR-cells, and low proliferation index. ACC32 cells presented an epithelioid morphology with higher nuclear atypia and prominent nucleoli. This tumor has few PgR IR cells with faint staining intensity with no ER expression and moderate proliferation index. ACC55 cells showed a solid growth composed of clusters of eosinophilic cells with frequent nuclear atypia and mitotic figures. This tumor has moderate PgR expression with negative ER immunostaining and a labeling index up to 15%. The ACC91 cells had a solid growth composed by poorly cohesive cell clusters with densely eosinophilic

cytoplasm, frequent nuclear atypia and mitosis. This tumor has a higher expression of PgR along with

| code   | PgR       |               |            | ER        |               |            |
|--------|-----------|---------------|------------|-----------|---------------|------------|
|        | intensity | % of IR cells | cumulative | intensity | % of IR cells | cumulative |
| ACC03  | 1         | 2             | 3          | 0         | 0             | 0          |
| ACC04  | 2         | 3             | 5          | 1         | 0             | 1          |
| ACC06  | 1         | 1             | 2          | 2         | 2             | 4          |
| ACC07  | 2         | 3             | 5          | 2         | 2             | 4          |
| ACC08  | 1         | 2             | 3          | 0         | 0             | 0          |
| ACC10  | 3         | 3             | 6          | 2         | 1             | 3          |
| ACC11  | 2         | 2             | 4          | 0         | 0             | 0          |
| ACC12  | 1         | 1             | 2          | 1         | 0             | 1          |
| ACC13  | 1         | 2             | 3          | 0         | 0             | 0          |
| ACC14  | 1         | 2             | 3          | 1         | 1             | 2          |
| ACC16  | 2         | 2             | 4          | 1         | 0             | 1          |
| ACC17  | 1         | 0             | 1          | 0         | 0             | 0          |
| ACC23  | 1         | 0             | 1          | 0         | 0             | 0          |
| ACC24  | 2         | 2             | 4          | 0         | 0             | 0          |
| ACC26  | 1         | 2             | 3          | 0         | 0             | 0          |
| ACC27  | 1         | 2             | 3          | 1         | 0             | 1          |
| ACC29  | 2         | 1             | 3          | 1         | 0             | 1          |
| ACC30  | 2         | 3             | 5          | 0         | 0             | 0          |
| ACC32  | 1         | 1             | 2          | 0         | 0             | 0          |
| ACC38  | 2         | 2             | 4          | 1         | 0             | 1          |
| ACC40  | 1         | 1             | 2          | 0         | 0             | 0          |
| ACC48  | 1         | 2             | 3          | 2         | 2             | 4          |
| ACC50  | 1         | 2             | 3          | 1         | 0             | 1          |
| ACC55  | 1         | 1             | 2          | 0         | 0             | 0          |
| ACC64  | 2         | 3             | 5          | 0         | 0             | 0          |
| ACC68  | 2         | 3             | 5          | 0         | 0             | 0          |
| ACC71  | 2         | 2             | 4          | 1         | 2             | 3          |
| ACC74  | 2         | 2             | 4          | 0         | 0             | 0          |
| ACC75  | 1         | 1             | 2          | 0         | 0             | 0          |
| ACC79  | 1         | 0             | 1          | 0         | 0             | 0          |
| ACC81  | 2         | 2             | 4          | 0         | 0             | 0          |
| ACC85  | 1         | 3             | 4          | 0         | 0             | 0          |
| ACC91  | 2         | 3             | 5          | 1         | 2             | 3          |
| ACC99  | 1         | 2             | 3          | 0         | 0             | 0          |
| ACC103 | 1         | 2             | 3          | 0         | 0             | 0          |

moderate expression of ER. Labeling index is higher between these samples, ranging from 15 to 20%.

Table 6. Histological features and expression of PgR and ER in ACC tumor specimens.

### **Progesterone exerts cytotoxic effects on ACC cells through autophagy-related apoptosis.**

We have previously demonstrated that Pg can induce a cytotoxic effect in each ACC cell models used here, even if with different effectiveness and potency [90, 92]. Preliminary results obtained with the acridine orange staining suggest that apoptosis could be induced by Pg in NCI-H295R cells. A time course of Pg exposure (24, 48, 72, or 96h) at its IC<sub>50</sub> was conducted using Annexin V/PI staining to detect apoptotic cell death induced by Pg in the experimental ACC cell models used in the present study. Figure 3 shows the results of the time-course experiments, from which a significant increase in apoptotic cells emerged, depending on the cell model examined. In NCI-H295R cells (Figure 3A), exposure to Pg confirmed a significant increase in apoptotic cells after 48h of treatment (apoptotic cells: untreated: 11.28 % ± 4.76%, Pg-treated: 27.95% ± 3.02%, p<0.05), confirming published results [92]. In MUC-1 cells (Figure 3B), Pg treatment induced a significant decrease in viable cells and a significant increase in apoptotic cell ratio after 72 and 96h of treatment (72 h viable cells: untreated: 96.13% ± 0.72%, Pg-treated cells: 79.25% ± 5.39%, p<0.01); (72 h apoptotic cells: untreated: 3.42% ± 0.86%, Pg-treated: 15.47% ± 2.21%, p<0.001); (96h viable cells: untreated: 92.91% ± 1.11%, Pg-treated: 78.58% ± 0.48%, p<0.0001); (96h apoptotic cells: untreated: 6.81% ± 1.13%, Pg-treated: 21.08% ± 0.64%, p<0.0001).

In MUC-1 cells, no significant increase in necrotic cells was observed. In the TVBF-7 cell line, no significant differences were observed, except for an increased percentage of viable cells after 96h of treatment (untreated viable cells: 83.69% ± 3.85%, Pg-treated viable cells: 95.90% ± 1.54%, p<0.05) (Figure 3C). To elucidate the death mechanism underlying the cytotoxic effect of Pg on TVBF-7 cells, we analyzed the expression of microtubule-associated protein light chain 3 (LC3) with particular attention to LC3-II, the maturation form of LC3-I, which can be used as a biomarker of autophagosome formation. Figure 4C showed that Pg induced autophagy on TVBF-7 cells with a significant increase in both LC3-I and LC3-II levels in a time-dependent manner. In NCI-H295R (Figure 4A) and MUC-1 (Figure 4B) cell lines, where apoptosis cell death was observed, a slight rise in LC3-I and LC3-II levels can be appreciated, although not significant and with a trend tending to decline.

These observations confirm that, in a complex interplay between autophagy and apoptosis pathways, apoptosis is promoted when autophagy is inhibited [182]. Taken together these results suggest that autophagy and apoptosis occur hierarchically or independently to contribute to Pg-induced ACC cell death.

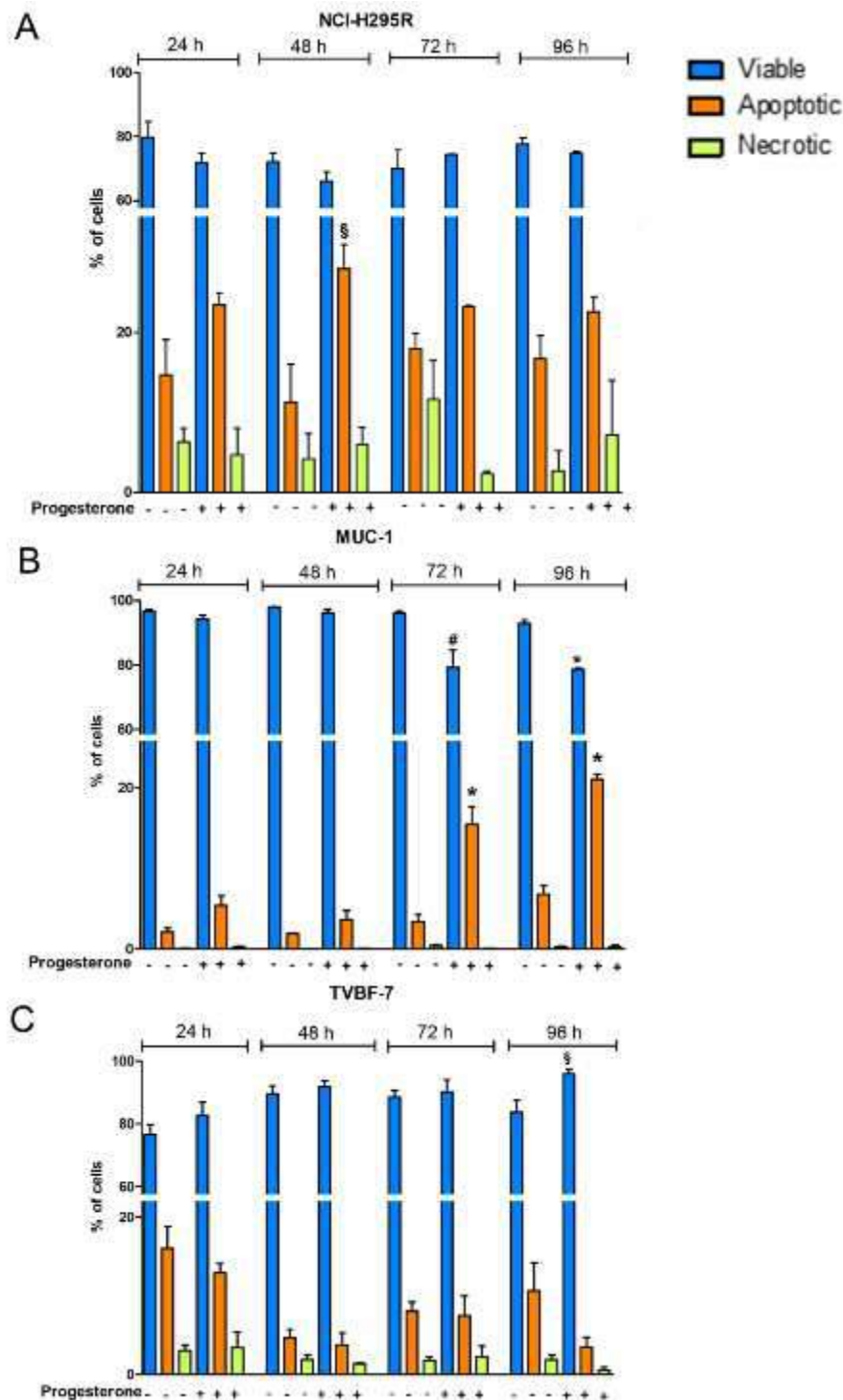


Figure 3. Progesterone promotes apoptotic cell death in NCI-H295R (A) and MUC-1 (B) cell lines but not in TVBF-7 cells (C). Cells were treated for 24, 48, 72, or 96h using their Pg IC50 values, stained with Pacific Blue™ Annexin V, and analyzed by flow cytometry. Histograms representative of the mean ± SEM of three experiments were shown. \* $p < 0.0001$ , # $p < 0.001$  cells, § $p < 0.05$  vs

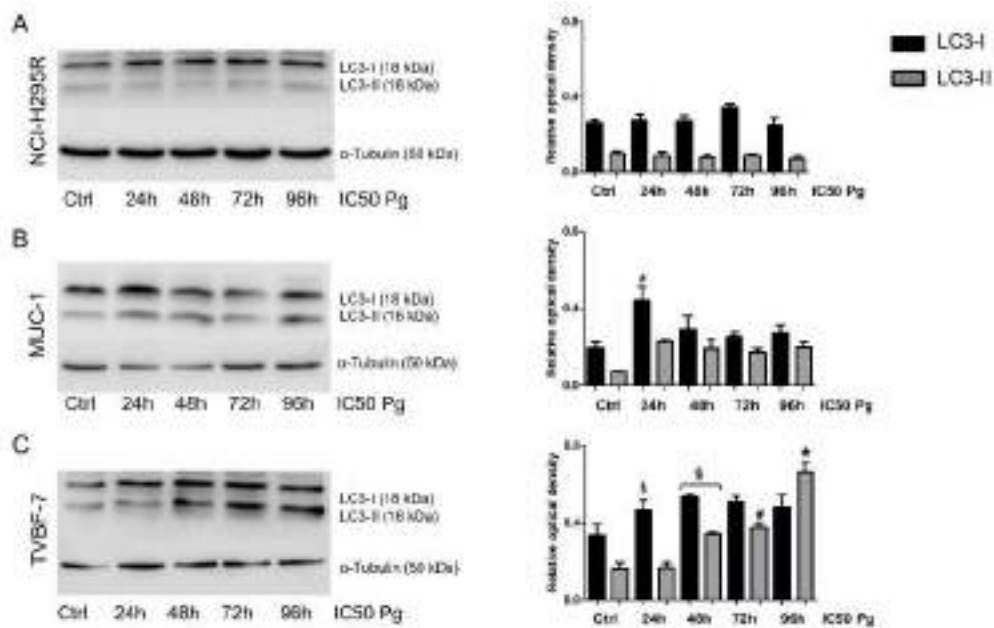


Figure 4. Progesterone triggers autophagy cell death in TVBF-7 cell lines. Representative Western Blot of LC3-I and LC3-II proteins levels in NCI-H295R (A), MUC-1 (B) and TVBF-7 (C) are shown. On the right side, quantification results are presented as a relative optical density means  $\pm$  SEM of three independent experiments. \* $p < 0.0001$ , # $p < 0.001$ , § $p < 0.05$  vs untreated cells.

### Progesterone induces changes in the cell cycle distribution.

To evaluate the effect of Pg administration on the cell cycle profile, the cell cycle distribution in ACC cell lines after Pg treatment for 72h and 96h was studied. Figure 5 A-B showed that, in NCI-H295R cells, treatment with Pg increased the proportion of cells in the G1 phase both after 72h and 96h. (72h:  $+10.65 \pm 4.1\%$ , 96h:  $+3.08 \pm 0.05\%$ ;  $p < 0.05$ ). An increase in the G2 phase fraction was observed in MUC-1 cells at the same time points (72h:  $+11.1 \pm 0.05\%$ , 96h:  $+8.18 \pm 1.42\%$ ;  $p < 0.005$ ) and a decrease of cells in the S phase after 96h of treatment ( $-7.2 \pm 1.02\%$ ,  $p < 0.005$ ). No changes in the cell cycle distribution were observed in Pg-treated TVBF-7 cells compared to controls.

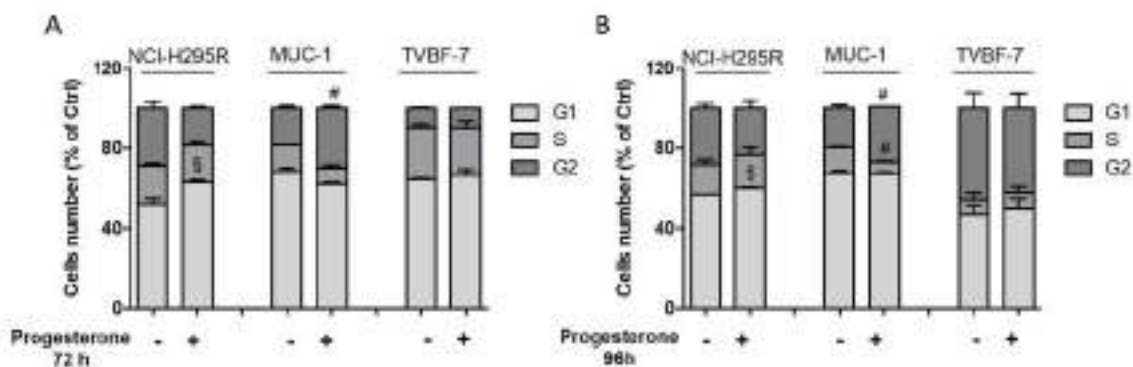


Figure 5. Progesterone induces changes in the cell cycle distribution of ACC cell lines. Cells were treated for 72 h (A) and 96h (B) with respective IC50 values of Pg, stained with propidium iodide, and analyzed for DNA



*content by flow cytometry. Histograms representative of the mean  $\pm$  SEM of three experiments were shown. #  $p < 0.001$ , § $p < 0.05$  vs untreated cells.*

### **Progesterone exerted a cytotoxic effect that was maintained after the drug is withdrawn.**

To evaluate whether the cytotoxic effect of Pg was a permanent effect even after the suspension of the treatment, the cells were treated with the respective  $IC_{50}$  values for 4 days and thereafter kept in culture for another 10 days in a complete, drug-free medium. Cell viability was evaluated at the end of treatment and at different times after discontinuation, as shown in Figure 6. The effect of Pg on NCI-H295R cells lasted up to 2 days after withdrawal. Cells then recover from the cytotoxic insult and the cell viability after 10 days of withdrawal was similar to untreated cells (Figure 6A). In MUC-1 cells, Pg induced cell damage, leading to cell death, with an effect that was maintained after drug discontinuation (Figure 6B). Interestingly, cell viability significantly continued to decrease up to 10 days after drug withdrawal ( $-83.2 \pm 1.5\%$  compared to untreated cells,  $p < 0.0001$ ). Figure 6C shows the effect of the drug withdrawn in TVBF-7 cells. Even if the cells seemed to slowly recover, the reduction of the cell viability remained significant ( $-39.4 \pm 2.07\%$  compared to untreated cells;  $p < 0.0001$ ).

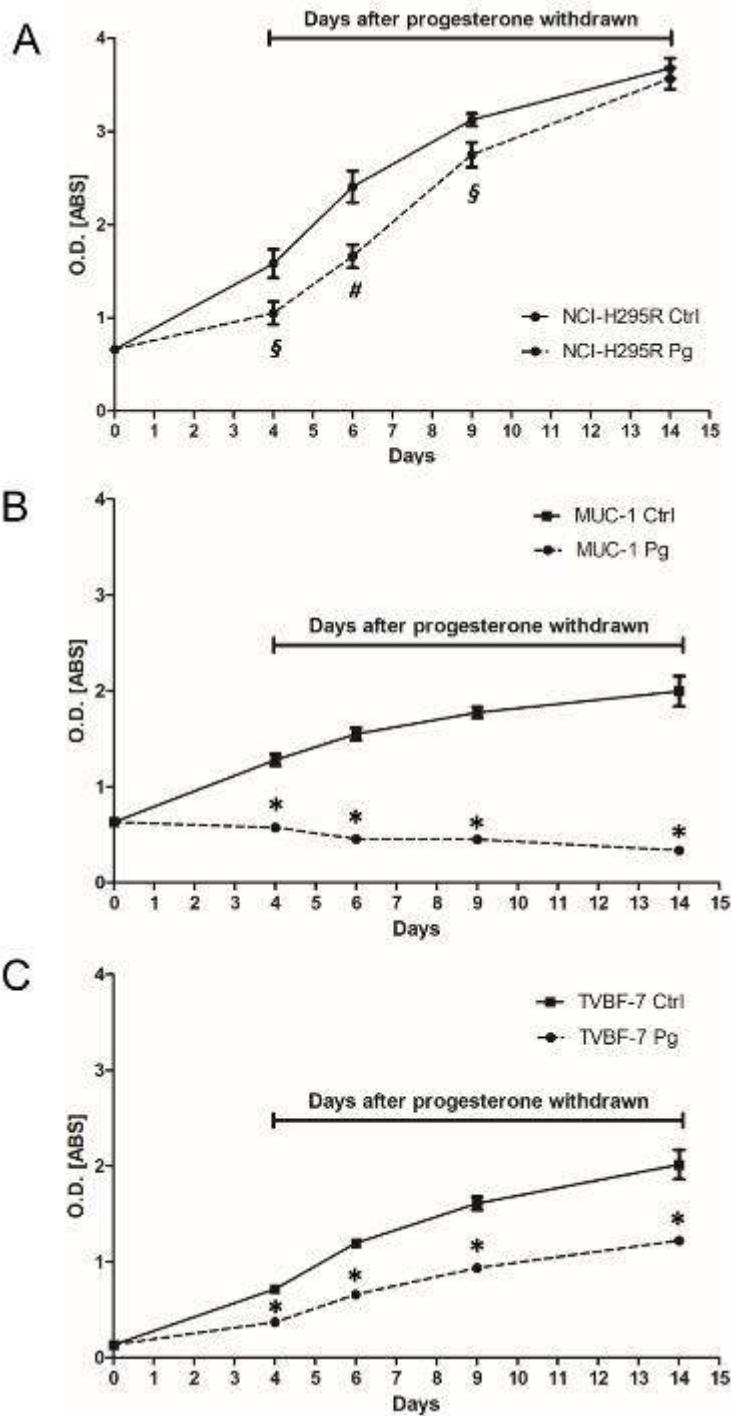


Figure 6. Effect of drug withdrawal on NCI-H295R (A), MUC-1 (B), and TVBF-7 (C) ACC cell lines. Cells were treated for 4 days with respective IC50 values of Pg and then the drug was withdrawn from the medium, and cells were kept in culture for a further 10 days. Cell viability was measured at the indicated times by the MTT assay. Points represent the mean  $\pm$  SEM of at least three experiments performed in triplicate. \* $p < 0.0001$ , # $p < 0.001$ , § $p < 0.05$  vs untreated cells.

## **Progesterone inhibits tumor growth and metastasis formation in the zebrafish/ tumor xenograft model**

We then evaluated the effects of Pg on ACC cell growth *in vivo*, in the ACC cell xenografted in kdrl-GFP zebrafish embryos model. Preliminary experiments were conducted to evaluate the Pg toxicity on wild-type (AB) strain zebrafish embryos. Doses higher than 50  $\mu\text{M}$  caused 100% mortality. Exposure to 25  $\mu\text{M}$  Pg was not lethal, but nearly 50% of embryos developed pericardial edema and yolk sac edema. Lowering Pg doses down to 10  $\mu\text{M}$ , the drug did not induce side effects in zebrafish embryos. Based on these results, the concentrations of 6.25  $\mu\text{M}$  and 12,5  $\mu\text{M}$  were chosen to evaluate the effects of Pg on ACC cells growth in the xenografted zebrafish model. Figure 7 (A-B) shows the results obtained by exposing embryos to 6.25  $\mu\text{M}$  Pg demonstrating that Pg was able to significantly reduce the tumor mass in each cell line (NCI-H295R:  $-30.15\% \pm 7.22\%$ ,  $p < 0.05$ ; MUC-1:  $-41.5\% \pm 10.47\%$ ,  $p < 0.0001$ ; TVBF-7:  $-34.03\% \pm 4.28\%$ ,  $p < 0.0001$ ). When embryos were treated with 12.5  $\mu\text{M}$ , we observed a high mortality rate in embryos xenografted with MUC-1 cell line and a significant reduction of tumor area in those injected with NCI-H295R ( $-46.48\% \pm 4.82\%$ ;  $p < 0.0001$ ) and TVBF-7 ( $-37.53\% \pm 2.15\%$ ;  $p < 0.0001$ ) cell lines (not shown). Furthermore, according to their metastatic origin, MUC-1 and TVBF-7 cells were found to be able to metastasize, though with some differences in terms of rate and metastatic localization (Figure 8). No metastases were observed in embryos xenografted with NCI-H295R cells, in line with their origin from a primary ACC. Pg was able to reduce the rate of embryos with MUC-1 cells migrating to the caudal region from  $62,5 \pm 9,6\%$  to  $10,8 \pm 0,85\%$  ( $p < 0.05$ ). TVBF-7 cells were able to form metastasis at a lower rate, compared with MUC-1 cells (metastasis-positive embryos:  $12.07\% \pm 7.31\%$ ), and metastasis was mostly localized in the pericardial zone. No embryos with metastasis were found in the Pg-treated group. Collectively, these data indicated that Pg suppressed ACC cells growth and metastasis formation in *in vivo* model.

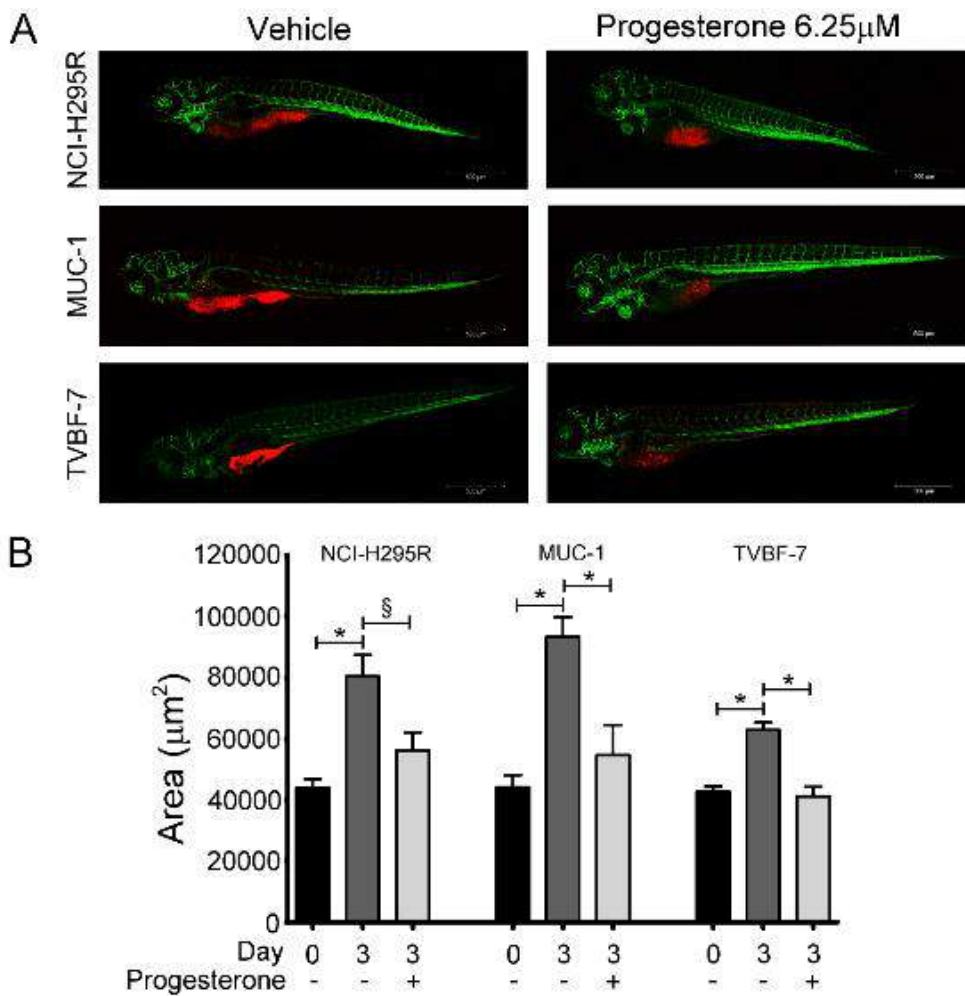


Figure 7. Progesterone induced a reduction of the tumor xenograft area of ACC cells. (A) Representative, lateral-view pictures of Tg(kdrl:EGFP) control and Pg-treated embryos at 120 hpf. All three cell lines are labeled with a red fluorescent lipophilic dye while the embryos' endothelium is labeled with a green fluorescent protein reporter driven by the kdrl promoter. Images were acquired using a Zeiss LSM 510 META confocal laser-scanning microscope at 10x magnification. (B) Tumor areas of 48 hpf (T0 - start of treatment) and 120 hpf (T3 - end of treatment) of drug-treated and vehicle-treated groups were measured using Zen 2.3 Black software from ZEISS. Data are shown as mean of independent experiments  $\pm$  SEM. \* $p < 0.0001$ ;  $\$p < 0.05$ .

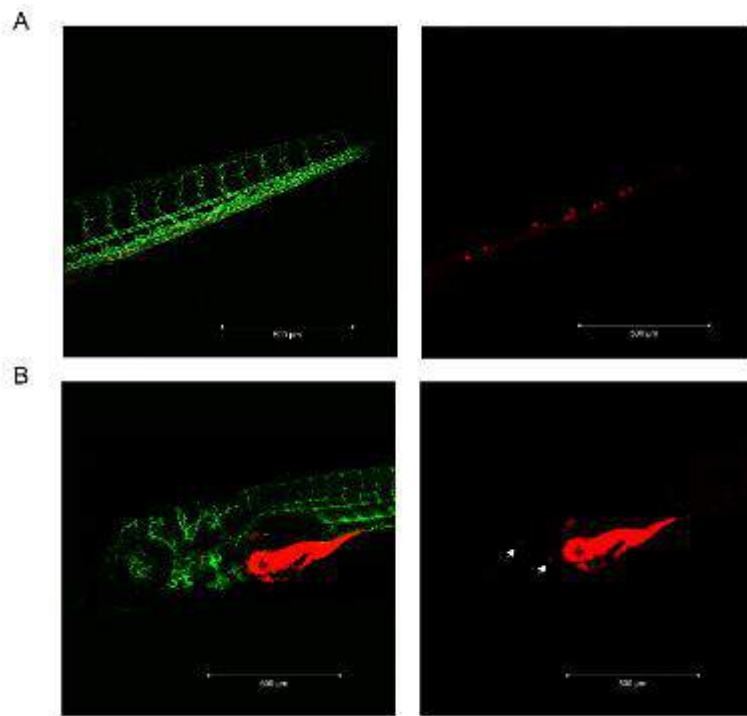


Figure 8. MUC-1 and TVBF-7 ACC cells induced metastasis formation in zebrafish embryos. (A) Enlargement of the embryo tail with metastasized MUC-1 cells. (B) A representative acquisition of the metastases of TVBF-7 cells in the pericardial area of the embryo is shown. Cells are labeled with a red fluorescent lipophilic dye while the embryos' endothelium is labeled with a green fluorescent protein reporter driven by the *kdrl* promoter. Images were acquired at 120 hpf using a Zeiss LSM 510 META confocal laser-scanning microscope at 10x magnification.

### Progesterone suppresses the migration and invasion ability of ACC cells

To confirm the results obtained in the zebrafish model, we decided to further investigate the motility of ACC cells using *in vitro* approaches such as the transwell and wound healing assays. Figure 9 shows the effect of Pg on the invasion and migration ability of each ACC cell lines with some representative images.

MUC-1 cells displayed a high invasive capability, confirming the results obtained in the zebrafish models. The invasion and migration ability of MUC-1 cells were strongly reduced by Pg ( $-49.42 \pm 5.34\%$  invasive cells,  $p < 0.005$ ;  $-42.76 \pm 1.17\%$  migrated cells,  $p < 0.0001$ ; cell separation distance:  $421.7 \mu\text{m} \pm 16.64 \mu\text{m}$  in Pg-treated cells vs  $303.1 \mu\text{m} \pm 18.61 \mu\text{m}$  in untreated cells,  $p < 0.0001$ ). A similar anti-metastatic effect of Pg was observed in TVBF-7 cells, confirming also *in vitro* results obtained *in vivo*, showing a low invasion ability ( $-36.85\% \pm 7.83\%$  invasive cells,  $p < 0.05$ ;  $-62.29\% \pm 16.28\%$  migrated cells,  $p < 0.05$ ). The transwell migration assay revealed an even lower ability to migrate compared to the ability to invade. The purely technical reason may lie in the less

incubation time used for migration assay (22h for migration assay and 72h for invasion assay, as indicated in the manufacturer's protocols). On the other side, the wounding assay proved that TVBF-7 cells could migrate and that Pg hindered the edges reconnection (cell separation distance:  $606.7 \mu\text{m} \pm 9.14 \mu\text{m}$  in Pg-treated cells vs  $480.9 \mu\text{m} \pm 14.13 \mu\text{m}$  in untreated cells,  $p < 0.0001$ ).

In line with the previous observations, NCI-H295R showed a limited ability to migrate or to invade that was not significantly modified by Pg treatment.

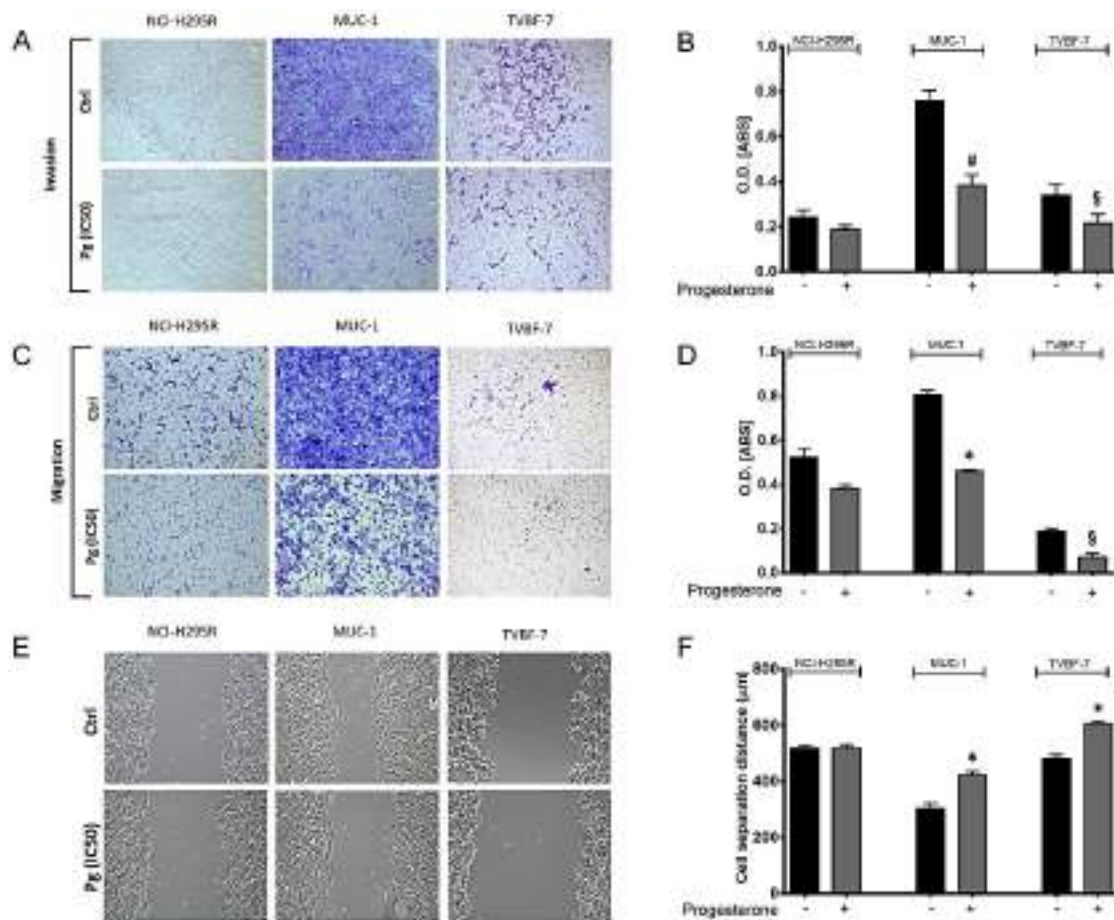


Figure 9. Progesterone suppresses ACC cells' invasion (A) and migration (C) ability in transwell assays. (B, D) Quantification of the number of invasive and migrated cells was analyzed using the absorbance of the staining detected at 560nm. (E) Representative images of wound-healing assay used to detect migrated ACC cells. (F) The distance between each edge of the scratch was measured using NIH ImageJ Software. Images were acquired using an Olympus IX51 optical microscope equipped with a 10x objective. Data are shown as mean  $\pm$  SEM. \* $p < 0.0001$ , # $p < 0.001$ , § $p < 0.05$  vs untreated cells.

## Pg interferes with metalloprotease 2 (MMP-2) Activity

The activity of metalloproteases is crucial for the cell invasion process [183]. Among these, ACC tissues specifically express high levels of MMP-2 compared to normal adrenal tissues, representing an unfavorable prognostic factor [184]. Our preliminary qRT-PCR analysis on MMPs expression (Table 7) confirmed that on ACC cell lines the most expressed is MMP2, even if at different levels between NCI-H295R and the metastatic cell lines (Table 8).

**Table 7. MMPs gene expression in ACC cell lines**

|             | NCI-H295R    | MUC-1       | TVBF-7       |
|-------------|--------------|-------------|--------------|
| MMP10       | 14,96        | 14,56       | 16,34        |
| MMP11       | 11,70        | 10,12       | 15,08        |
| MMP13       | 17,78        | 11,81       | 18,68        |
| <b>MMP2</b> | <b>10,71</b> | <b>7,19</b> | <b>7,71</b>  |
| MMP3        | 14,73        | 15,28       | 14,62        |
| MMP7        | 19,48        | 12,06       | Undetermined |
| MMP9        | 10,77        | 10,16       | 11,37        |

Values were reported as  $\Delta Ct$  that are differences of the threshold cycle (Ct) values between the gene of interest and the average of three different housekeeping genes, included into the Human Tumor Metastasis RT2 Profiler PCR Array.

Based on this observation, we evaluated whether Pg could modify MMP2 expression and secretion. No significant differences were observed in MMP2 gene expression as well as in its inhibitors (TIMP1 and TIMP2) after treatment in all three cell lines (Table 8).

**Table 8. MMP2 and its inhibitors gene expression in ACC cell lines**

| Target gene | Basal expression levels |           |           | Expression levels after Pg-treatment |           |           |
|-------------|-------------------------|-----------|-----------|--------------------------------------|-----------|-----------|
|             | NCI-H295R               | MUC-1     | TVBF-7    | NCI-H295R                            | MUC-1     | TVBF-7    |
| MMP2        | 11.01±0.48              | 7.74±0.1  | 7.47±0.1  | 11.14±0.17                           | 8.41±0.07 | 7.55±0.05 |
| TIMP1       | 5.98 ±0.32              | 7.74±0.09 | 6.80±0.22 | 5.59±0.17                            | 8.41±0.08 | 6.80±0.28 |
| TIMP2       | 5.44±0.28               | 2.52±0.16 | 9.24±0.06 | 4.77±0.22                            | 2.35±0.14 | 8.95±0.03 |

Values were reported as  $\Delta Ct$  that are differences of the threshold cycle (Ct) values between the gene of interest and  $\beta$ -actin housekeeping gene.

Western blot analysis, performed on conditioned media, revealed that Pg significantly reduced the secreted MMP2 levels compared to untreated cells in metastatic cell lines (Figure 10A). Figure 10B shows the zymography results for the activity of MMP-2 equally impaired by Pg treatment (Pg-treated MUC-1 cells  $-27.82 \pm 1.17\%$  vs untreated,  $p < 0.001$ ; Pg-treated TVBF-7 cells  $-24.19 \pm 4.43\%$ ,  $p < 0.05$ ). No significant differences were observed in MMP-2 levels and activity after treatment on NCI-

H295R cells. The low MMP2 levels observed in NCI-H295R cells compared with metastatic cell lines, are in line with their primitive origin and lack of capability to invade both *in vitro* and *in vivo* models. These results strengthen the involvement of MMP-2 in the progression and invasiveness of ACC.

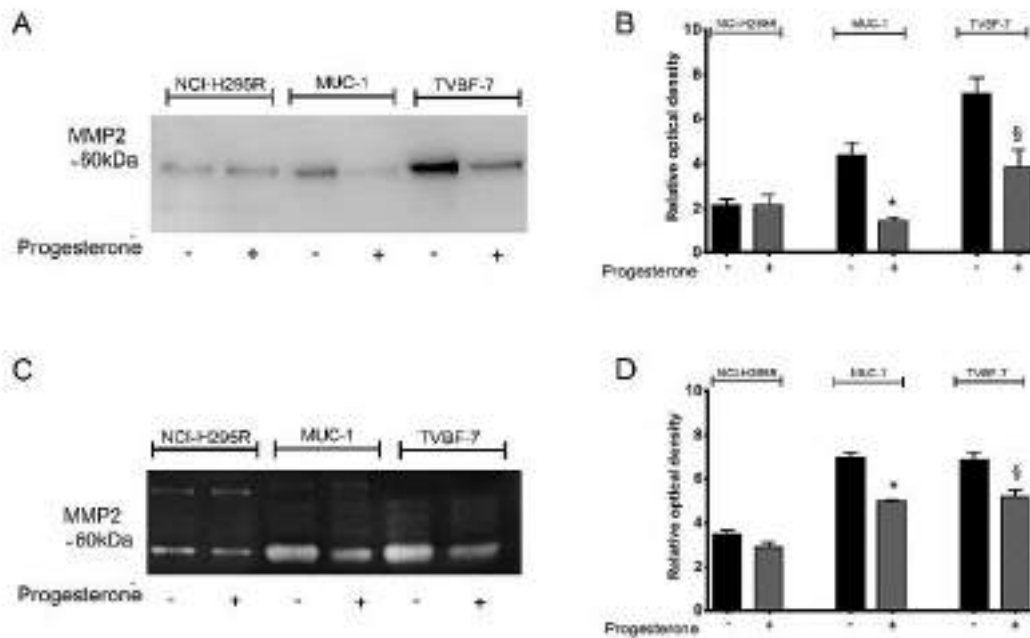


Figure 10. The secretion and the activity of MMP 2 were decreased after Pg treatment. (A) Representative western blot of MMP2 in the conditioned medium secreted by ACC cells. (C) Representative zymogram of MMP2 in the conditioned medium secreted by ACC cells. (B, D) Quantification of western blots and zymography. Results are presented as a relative optical density means  $\pm$  SEM of three independent experiments. \* $p < 0.0001$ , § $p < 0.05$  vs untreated cells



## 6.2 Results Part II: Potential role of WEE1 inhibitor in ACC

### WEE1 expression in ACC tissues and correlation of WEE1 staining with clinicopathological parameters.

WEE1 expression on adrenal tissues was evaluated both at mRNA and protein levels. qRT-PCR analysis revealed that relative *WEE1* expression was significantly higher in ACC compared to NAG (median levels 0.032 vs 0.012,  $p=0.049$ ) but not to ACA (Figure 11A). The median value of *WEE1* expression (0.032) was used as cut-off to define low and high expression. At multivariate analysis, low WEE1 mRNA levels were associated with better overall survival (HR 0.32, 95%CI 0.12-0.86,  $p=0.02$ ) independently of established prognostic factors, including ENSAT tumor stage, resection status, Ki67% and hormone secretion (Figure 11B). No other correlation with clinical parameters were found.

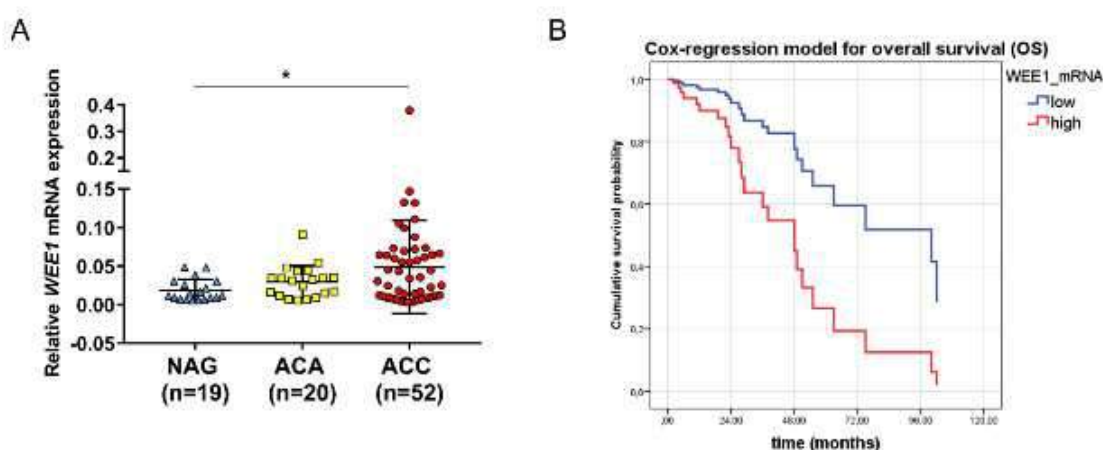


Figure 11. (A) Relative *WEE1* mRNA expression in adrenocortical tissues. (B) Association between *WEE1* expression and overall survival.

WEE1 staining was considered positive when localized to the nucleus. Median WEE1 nuclear staining was scored 79 (range 14-241).

*TP53* germline or somatic mutation was found in 34 out 114 (29.8%) cases, whereas the remaining cases were *TP53* wild type. Interestingly, WEE1 nuclear staining was significantly higher in *TP53* mutated samples compared to wild type (median score 97 vs 72,  $p<0.001$ ) (Figure 12 A). Moreover, endocrine inactive tumors had significantly higher WEE1 staining compared to glucocorticoid secreting ACC (median score 102 vs 67,  $p=0.003$ ), whereas no difference was observed comparing with other hormone secretion (Figure 12 B). A positive significant correlation, although weak, was

found between WEE1 and Ki67 as shown in Figure 12 C. No other correlations were found between WEE1 staining and other clinical parameters. Using the median score as cut-off, we divided our cohort in low (score <79) and high (score  $\geq$ 79) WEE1 staining. We observed any correlation with OS (median OS 81 vs 79 months in low and high WEE1, respectively,  $p=0.85$ ) and PFS (median PFS 16 vs 8 months in low and high WEE1, respectively,  $p=0.85$ ).

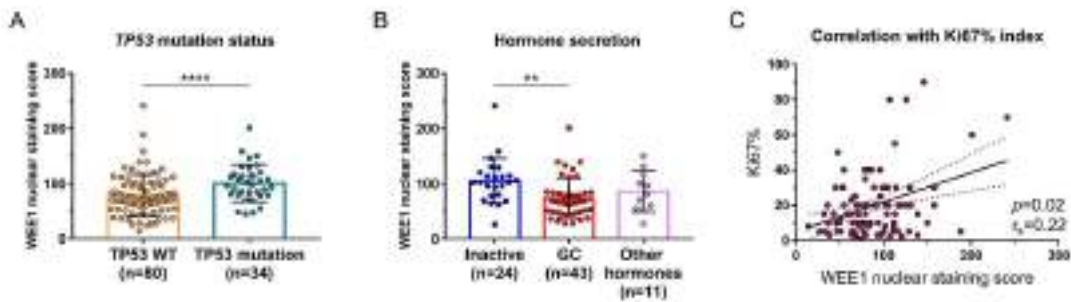


Figure 12. Correlation of WEE1 staining with clinicopathological parameters.

### Effect of adavosertib on ACC cell lines

We then evaluated the effects of the WEE1-inhibitor adavosertib on cell viability using five different ACC cell lines: NCI-H295R, MUC-1, JIL-2266, CU-ACC1 and CU-ACC2. Their mutation status is shown in Table 7. WEE1 expression was evaluated in ACC cell models both at mRNA and protein levels. Results, reported in Figure 13, shown a variable expression of WEE1 among the five analyzed cell lines with CU-ACC1 cells presenting the lowest expression both at mRNA and protein levels.

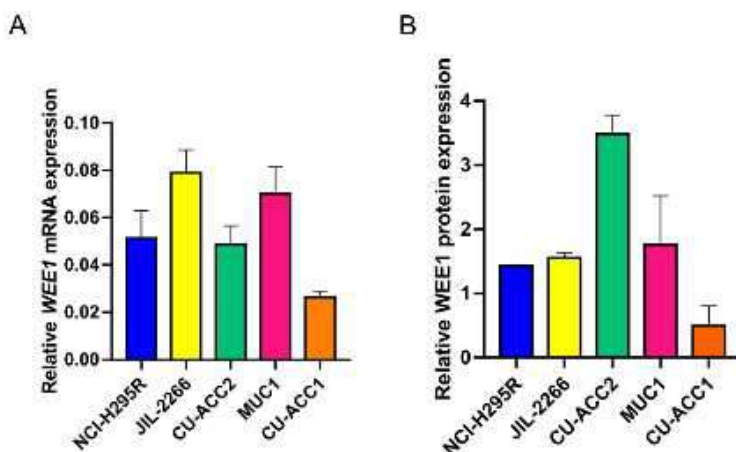
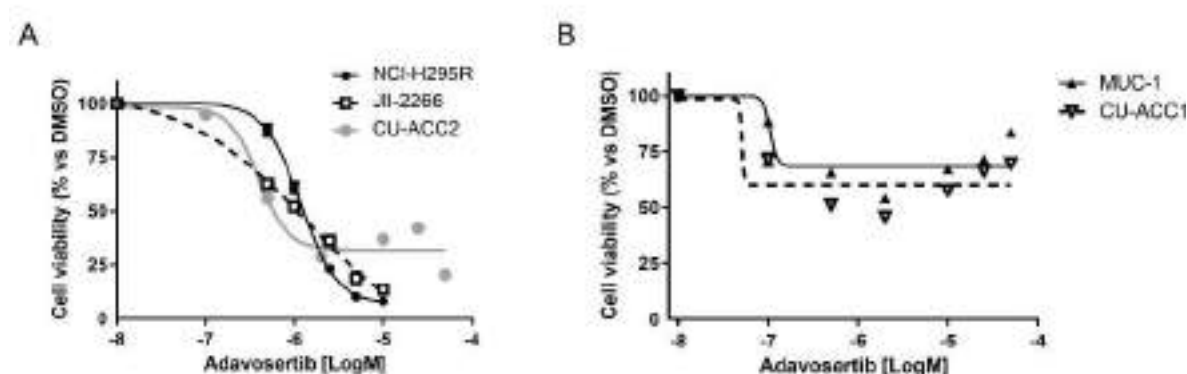


Figure 13. Relative expression of WEE1 at mRNA (A) and protein levels (B) in ACC cell lines.

**Table 9.** Known mutations of ACC cell lines [176]

| Cell line        | Mutation  |
|------------------|---|
| <b>NCI-H295R</b> | Homozygous deletion of exons 8–9 of the <b>TP53</b> gene<br>Activating mutation on CTNNB1 gene (p.S45P)   |
| <b>MUC-1</b>     | Somatic mutation in <b>TP53</b> gene<br>(deletion/ frameshift: NM_000546:c.1024delC – p.R342fs).  |
| <b>CU-ACC1</b>   | Mutation on CTNNB1 gene (p.G34R)  |
| <b>CU-ACC2</b>   | Mutation on <b>TP53</b> gene (p.G245S)<br>Mutation on MSH2 gene (exons 1-6 deletion)  |
| <b>JIL-2266</b>  | Hemizygous mutation on <b>TP53</b> gene<br>(NM_000546.5:exon8:c.859G>T: p.E287X).<br>Mutation on MUTYH gene (NM_012222.2:exon3:c.316C>T: p.R106W)<br>mutation identified in patient and the derived cell lines. |

To explore the possible involvement of WEE1 in ACC cytotoxicity, ACC cells were treated with increasing concentrations of adavosertib (0.01-100  $\mu$ M) for 4 days and then evaluated for cell viability. The ACC cell line NCI-H295R, JIL-2266, and CU-ACC2 displayed a concentration-dependent cytotoxicity, with the IC50 of 1.175, 1.35 and 0.4  $\mu$ M, respectively (Figure 14A). MUC-1 cell line and CU-ACC1 cells resulted resistant to adavosertib (Figure 14B), consistent with the lower WEE1 expression in these ACC cell models.



*Figure 14. Cytotoxic effect of adavosertib in sensitive (A) and resistant (B) ACC cell models. Cells were treated with increasing concentrations of adavosertib (0.1–100  $\mu$ M), then cell viability was analyzed by Glo assay. Data are expressed as percent of viable cells vs DMSO. Data are the mean  $\pm$  SEM of three independent experiments.*

#### Effect of drug combined treatment on ACC cell viability

Since WEE1 inhibition may cause replication stress [122] and sensitize tumors to DNA-damaging therapies [185, 186], we evaluated whether the treatment with adavosertib could be enhance the cytotoxic effect of cisplatin or gemcitabine, equally known to interfere with replication and induce damage to DNA. The combined treatments were performed as described in material and methods.

The analysis revealed a prevalent additive/synergic effect when adavosertib was combined with cisplatin or gemcitabine in all evaluated cell lines (not shown).

### 6.3 Results Part III: potential role of FGF/FGFR pathway in ACC

#### FGFR expression and cytotoxic effect of FGFR inhibitors on ACC cell models

Several studies suggested that FGF/FGFR pathways are potentially interesting therapeutic targets [158, 159] in ACC.

Therefore, the aim of this project was to evaluate the in vitro cytotoxic and antiproliferative effects of drugs inhibiting the FGF/FGFR pathway, alone and in combination with established ACC chemotherapeutic drugs. Before starting the experiments, we looked at the different FGFRs expression in the available ACC cell lines, and at the current active or completed clinical trials (Clinicaltrials.gov, last update January 30th, 2022) that investigate the use of different FGFR inhibitors in several solid tumors with FGFR genomic alterations.

Table 10 shown the results regarding the expression of FGFRs in ACC cell lines.

Table 10. FGFRs gene expression in ACC cell lines

|                   | NCI-H295R          | MUC-1               | JIL-2266            | TVBF-7             | CU-ACC2            | CU-ACC1            |
|-------------------|--------------------|---------------------|---------------------|--------------------|--------------------|--------------------|
| <b>FGFR1 IIIB</b> | 14,35 ± 0,25       | 18,26 ± 0,18        | 16,54 ± 0,17        | 18,56 ± 0,24       | 16,44 ± 0,17       | 18,82 ± 0,41       |
| <b>FGFR1 IIIC</b> | <b>2,65 ± 0,23</b> | <b>4,45 ± 0,10</b>  | <b>4,945 ± 0,06</b> | <b>5,98 ± 0,53</b> | <b>5,82 ± 0,34</b> | <b>7,15 ± 0,15</b> |
| <b>FGFR2 IIIB</b> | <b>9,60 ± 0,10</b> | 11,27 ± 0,10        | 16,14 ± 0,51        | <b>5,10 ± 0,02</b> | 18,28 ± 0,06       | <b>8,28 ± 0,05</b> |
| <b>FGFR2 IIIC</b> | <b>7,78 ± 0,14</b> | <b>9,25 ± 0,065</b> | 14,6 ± 0,093        | <b>4,08 ± 0,32</b> | 16,5 ± 0,08        | <b>6,43 ± 0,11</b> |
| <b>FGFR4</b>      | <b>8,84 ± 0,4</b>  | 13,72 ± 0,14        | 14,4 ± 0,1          | <b>6,35 ± 0,06</b> | 12,91 ± 0,35       | <b>9,89 ± 0,16</b> |

*Values were reported as  $\Delta Ct$  that are differences of the threshold cycle (Ct) values between the gene of interest and  $\beta$ -actin housekeeping gene.*

All six cell lines showed weak levels of FGFR IIIb and high levels of FGFR1 IIIc isoform with NCI-H295R cells that expressed the highest levels ( $\Delta Ct$ : 2,65 ± 0,23; p<0.0001) and CU-ACC1 with the lowest levels ( $\Delta Ct$ : 7.15 ± 0.15; p<0.0001).

TVBF-7 cells showed a particular expression pattern with highest the levels of FGFR2 IIIb ( $\Delta Ct$ : 5,10 ± 0,02; p<0.0001), FGFR2 IIIc ( $\Delta Ct$ : 4,08 ± 0,32; p<0.0001) and FGFR4 ( $\Delta Ct$ : 6,35 ± 0,06; p<0.0001), followed by CU-ACC1 and NCI-H295R cells. (Table 10).

In MUC-1, JIL-2266 and CU-ACC2 cells lower and variable levels of both FGFR2 isoforms and FGFR4 can be found.

Among the FGFR-inhibitors, we chose erdafitinib and rogaratinib, which are pan-FGFR inhibitors with potential antineoplastic activity already used for urothelial carcinoma, and fisogatinib that is a selective FGFR4 inhibitor.

Exposure of NCI-H295R, MUC-1, JIL-2266, CU-ACC2 and TVBF-7 cells to increasing concentration of each drug induced cytotoxicity (Figure 15) with IC<sub>50</sub> values shown in the Table 11. The experiments are still ongoing to also evaluate the effect of these drug on CU-ACC1 cells.

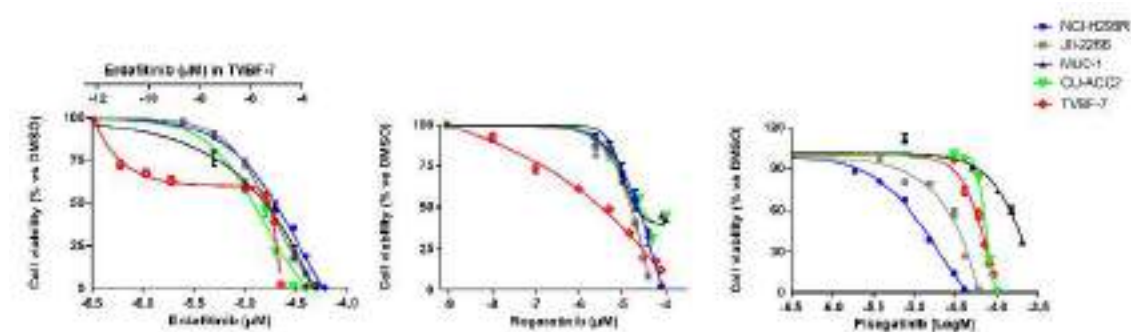


Figure 15. Cytotoxic effect of erdafitinib, rogaratinib and fisogatinib on ACC cell models. Cells were treated with increasing concentrations of each drug, then cell viability was analyzed by Glo assay. Data are expressed as percent of viable cells vs DMSO. Data are the mean ± SEM of three independent experiments.

|                  | <b>Erdafitinib</b> | <b>Rogaratnib</b> | <b>Fisogatinib</b> |
|------------------|--------------------|-------------------|--------------------|
| <b>NCI-H295R</b> | 17.93 μM           | 19.32 μM          | 10.7 μM            |
| <b>MUC-1</b>     | 25 μM              | >20 μM            | 84.16 μM           |
| <b>JIL-2266</b>  | 14.47 μM           | 12.58 μM          | 27.36 μM           |
| <b>CU-ACC2</b>   | 15.5 μM            | >20 μM            | 70.4 μM            |
| <b>TVBF-7</b>    | 0.1 μM             | 0.78 μM           | 70.2 μM            |

Table 11. IC<sub>50</sub> values of FGFR-inhibitors in ACC cell lines.

All 5 cell lines displayed concentration-dependent cytotoxicity of erdafitinib, with TVBF-7 cells that are the most sensitive (IC<sub>50</sub> value of 0.1 μM) and MUC-1 cells the less sensitive (IC<sub>50</sub> value of 25 μM).

Rogaratinib exerted a cytotoxic effect in a concentration- dependent manner in all used cell lines. As for the erdafitinib, TVBF-7 were the most sensitive also to rogaratinib (IC<sub>50</sub> value of 0.78 μM). Fisogatinib exposure did not show any effect on cell viability up to 50 μM except on NCI-H295R and JIL-2266 cells, with IC<sub>50</sub> values of 10.7 and 27.36 μM respectively.

## 7. Discussion

ACCs are often highly aggressive and poor prognosis tumors. Besides usually being detected in advanced stages, one of the reasons for an unfavorable outcome of patients with adrenal cancer is also the absence of effective treatment options.

In recent years, unprecedented progresses in cancer biology and genomics have fostered the development of numerous targeted therapies for various malignancies. Immunotherapy, for example, has transformed the treatment landscape of malignancies such as melanoma, among others. However, these advances have not brought meaningful benefits for patients with ACC. Thus, identifying new therapeutic strategies in ACC continues to be a major challenge.

Among the different therapeutic targets expressed in ACC, we focused our attention on the druggable role of the Pg/PgR and E/ER pathways as well as on the WEE1 kinase. Finally, an emerging role for the FGF/FGFR pathway alteration was observed in different cancers, including ACC [147].

Thus, this thesis aimed to evaluate the role of each of the above-indicated pathways, trying to demonstrate whether the modulation of their activity could exert cytotoxic/antiproliferative effects in the different human ACC cell models now available. This is an important point as the scarcity of human ACC cell lines hampered more detailed preclinical investigations in the past and the development of strategies considering, for example, various genotypes, secretion profiles, and drug-resistant phenotypes. However, since 2016, tremendous progress in this field has been observed, with five new human adrenocortical cell lines developed to give researchers instruments that cover the well-known heterogeneity of this disease and have the potential to reveal so far unknown patient subtype characteristics. Furthermore, ACC cell lines of metastatic origin can offer useful models to investigate the pharmacological effect of drugs and the pathological molecular alteration in the context of metastatic and EDP-M-progressed disease, which is specifically challenging in clinic management and closely related to poor prognosis.

We thus firstly investigated *in vitro* whether the interplay between ER, PgR, and their ligands may exert a cytotoxic and antiproliferative activity on ACC experimental cell models, as it was demonstrated in endocrine-related cancers.

Although the ER expression was relatively low, tamoxifen exerted cytotoxic effect on NCI-H295R cell line, belonging from a primary ACC, confirming published data [89]. However, the role of ERs in ACC cell models seemed to be limited to the NCI-H295R cell line, as the more recently



established human cell lines derived from metastatic cancer, such as MUC-1 and ACC115m/TVBF-7 expressed very weak levels of both ER subtypes and were resistant to tamoxifen.

On the same line, this mechanism may have a scarce impact in clinic, as our immunostaining data showed that ER is scarcely expressed in paraffin-embedded ACC tissues as well as we observed in ACC experimental cell models, accordingly with those that detected low expression level of the ER subtypes in ACC.

Concerning PgR, immunohistochemical analysis of ACC tissues strongly indicated that they are frequently expressed, with a few samples displaying a high percentage of immunoreactive cells, although with a large variability among samples. Accordingly, in a recent paper, our group demonstrated that exposure to Pg of primary cells derived from PgR expressing ACC (at least 40% of PgR+ cells) resulted in a concentration-dependent increase of cytotoxicity [92], suggesting the possibility to evaluate their potential as another pharmacological tool in addition to the usual systemic therapy. Indeed, the use of bioidentical Pg formulations or synthetic compounds has been linked to lower rates of uterine and colon cancers and turned out to be useful in treating endometrial carcinoma, ovarian carcinoma, melanoma, mesothelioma, and prostate tumors [103].

Our results indicate that Pg is effective in inducing a cytotoxic effect in several cell models of ACC, although at lower potency in metastatic ACC cell lines compared to the NCI-H295R cell line. This effect seems to be strictly related to the level of PgR expression since the lower potency could be due to the lower PgR expression in metastatic lines compared to H295R cells [90]. Thus, the evaluation of the PgR expression during the pathological staging could be of interest to stratify the patients in a view to personalized medicine.

The cross-talk between ER/PgR was detectable both at physiological and pathological levels in endocrine tissues and tumors [187] and it has been suggested that the combined treatment using drugs targeting ER/PgR could be useful, although the safety profile of the drug combination must be considered [187]. Based on this, we tested whether the combination could be useful in the ACC cell line that is sensitive to the cytotoxic effect of tamoxifen, namely NCI-H295R. Results however demonstrated that Pg and tamoxifen combined exert an antagonistic effect, thus suggesting that this pharmacological approach could not be pursued in ACC, on the light also of the scarce ER expression observed in ACC samples.

We then investigated the mechanism of action by which Pg, through its receptors, induces the cytotoxic effect, and whether this effect was maintained over time. We found that Pg induced G1-phase arrest in the cell cycle only in the NCI-H295R cell line, and G2-phase arrest in MUC-1 cells, culminating in apoptotic cell death. While the TVBF-7 cell line did not show any inhibition and, although a cytotoxic effect was present, no increase in apoptotic or necrotic cells was observed. This

opens the way to the presence of different regulatory mechanisms of cell growth inhibition in specific ACC cell types, supporting the well known heterogeneity observed in ACC [188].

The mechanism underlying the cytotoxic effect of Pg on TVBF-7, seemed to be linked to an increase in LC3-II levels, representing the activation of autophagy. The role of autophagy in the ACC context is challenging because it plays a double-edged role as a survival response to chemotherapeutic drugs, resulting in treatment failure, but also as an important mechanism underlying tumor cell suicide [189-191]. The cytoprotective function of autophagy is activated in many circumstances by suppressing apoptosis and this evidence justifies the observation of an increase in the cell viability in TVBF-7 cells exposed to Pg. However, we would like to underline that interminable autophagy has been shown to enhance anticancer drug-induced cell death [192]. Remarkably, this study demonstrated that Pg triggered cytotoxicity due to autophagy or apoptosis depending on the ACC cell type. Further studies are needed to detail the molecular features underlying this difference. However, it is known that Pg is able to induce both apoptosis [193, 194] or autophagy [112-114] depending on cellular contexts; accordingly, it was already known that Pg induces cell cycle modifications in cell lines derived from human tumors, with sometimes opposite results that depend on the tumor origin [195, 196].

Drug withdrawal experiments have equally shown variable results in the different ACC cell models. NCI-H295R cells were able to quickly recover after cytotoxic insult and restart to proliferate, while metastatic cell models, MUC-1 and TVBF-7 cells, kept a low proliferation rate, evident especially in MUC-1 cells. This *in vitro* result is especially relevant considering the possible clinical application of this treatment, in particular in patients with advanced ACC, in whom maintaining a cytotoxic effect with low proliferating cells, would represent a very important aspect.

The *in vivo* experiments, using the ACC xenograft in zebrafish embryos further strengthened the role of Pg in reducing ACC cell proliferation. by results obtained in the *in vivo* model of ACC cell lines xenografted in zebrafish embryos. This result is of particular interest, as the Pg concentration that induces a significant reduction in the tumor mass area of each ACC cell line is remarkably lower compared to the *in vitro* effective concentration. We speculated that Pg, being a lipophilic molecule, could accumulate in the zebrafish yolk sack, since it is rich in lipids needed to sustain its growth and survival in the first 5 life days. This hypothesis however needs to be demonstrated by measuring the Pg levels in the embryos. Although we are aware of the limitations of this model, it should be underlined that it is an useful tool for *in vivo* first drug screening [197], and it allowed us to demonstrate that Pg inhibited metastasis formation in zebrafish embryos xenografted with highly metastatic cell lines such as MUC-1 and TVBF-7. This is a very interesting result, due to the high metastatic capability of ACC in patients [198] and this finding was analyzed in more detail, using

different in vitro assays that demonstrated that Pg reduces migration and invasion in ACC cell lines, in line with that reported in other tumors [115, 116].

The dissemination of malignant neoplasms often requires the degradation of different components of the matrix and basement membrane. MMPs are responsible for the degradation of several extracellular matrix (ECM) components. There are over 20 recognized MMPs, each with specific substrate requirements and structural domains. Among these, MMP-2 and MMP-9 are two highly associated with tumor dissemination and invasiveness [199]. Among these, ACC tissues specifically express MMP-2 (as compared also to normal adrenal tissue), and the elevated MMP-2 expression in ACC is an unfavorable prognostic factor [184]. Based on this, we found that Pg impairs the secretion and the activity of MMP2, suggesting that it could mediate at least in part the effect of Pg in suppressing the invasion of metastatic ACC cells. Despite this, Pg has not influenced the gene expression of MMP2 and its inhibitors TIMP1 and TIMP2, letting us speculate that it may act at different levels on the process of MMP2 maturation and secretion. This mechanism is worth to be deepened with future studies.

In addition to the PgRs, another potential therapeutic target for ACC is WEE1, a tyrosine kinase that controls the cell cycle at the G2/M transition and S phase preventing entry into mitosis [120].

The selected WEE1 inhibition by adavosertib prevents the phosphorylation of CDK1, leading to mitotic entry in the presence of DNA damage. This premature mitotic entry precipitates mitotic catastrophe and cell death. The biological role of WEE1 in cancer cells is not fully understood. Most findings suggest that WEE1 act like oncogenes rather than tumor suppressors. It has been reported that WEE1 is frequently overexpressed in both solid and hematological tumors and a genome-wide CRISPR screen of 563 cancer cell lines showed that they are essential for the cell viability of almost all cell lines [200]. The dependency of cancer cells on WEE1 family proteins may be linked to the following mechanisms: (i) the high proliferation rate of cancer cells that follows the activation of driver oncogenes (e.g. RAS, MYC) needs to be sustained by a strong cell cycle regulation machinery; (ii) cancer cells frequently have inactivate p53, which is a key gatekeeper of G0/G1 and S phases and, as a consequence, the regulation of cell cycle is sustained entirely by the G2/M checkpoint; (iii) the over-expression of DNA damage response related kinases is fundamental to maintain a tolerable level of genetic instability, an intrinsic feature of cancer cells [201, 202] [119]. Therefore, it could be speculate that, once the malignant transformation process has been induced, WEE1 upregulation exerts a pro-tumorigenic functions, by securing a tolerable level of genomic instability to cancer cells.

Thus, we firstly evaluated the expression of WEE1 mRNA in adrenal tissues and, in line with publication in other tumors [200], we showed that *WEE1* is overexpressed at mRNA levels in ACC in comparison with ACAs and normal adrenal gland tissues.

It should be underlined that contrasting results are reported on the potential correlation between WEE1 expression and clinical outcome [203, 204]. In our cohort, we observed that *WEE1* expression correlated with overall survival only at mRNA levels, whereas no correlation was found at protein levels. However, it should be considered that the two evaluated cohort included different patients. Therefore, a direct correlation between these studies was not evaluable, also because it is known that levels of mRNA will not always reflect the level of the encoded protein.

Interestingly, WEE1 nuclear staining was significantly higher in *TP53* mutated samples compared to wild type. WEE1 may be particularly important in p53-deficient cancers since WEE1 inhibition may sensitize tumors with p53 deficiency to DNA-damaging therapies [185, 186] [205]. In our cohort, *TP53* mutations (considering both germline and somatic mutations) were observed in 29.8% of cases. To the best of our knowledge, this is the first study which investigated the WEE1 expression in relationship with *TP53* mutation in a large cohort of tumor samples.

Treating the different ACC cell lines with the WEE1 inhibitor adavosertib, we found that 3 out 5 cell lines, namely NCI-H295R, JIL-2266, and CU-ACC2, were sensitive to adavosertib and displayed a concentration-dependent cytotoxicity with the  $IC_{50}$  ranging from 0.4 to 1.35  $\mu$ M, while MUC-1 and CU-ACC1 cells resulted resistant to adavosertib, confirming also previous preliminary results of a study investigating extensive drug screening in NCI-H295R and MUC1 cells [188]. These results allowed us to hypothesize that response to treatment in ACC cell lines seems thus to be independent to the *TP53* mutational status, as the CU-ACC1 cells express wild-type *TP53* mutation and are resistant to adavosertib, as well as MUC1 cells, which harbor a *TP53* mutation. Nowadays, in addition to *TP53* mutation, other potential predictor biomarkers have been proposed to predict the response to adavosertib, including WEE1 expression, or Cyclin E1 (CCNE1) expression [206]. However, these findings were confirmed only in few studies, and are needed to be validated.

Taking together, these results suggest that, although a direct correlation cannot be established, the effective concentrations of adavosertib in the three sensitive cell lines were below the achievable plasma concentration (1000-5000 nmol/L) in clinical trials [128, 207], thus suggesting a potential future clinical studies.

Up to now, the chemotherapy strategy in metastatic ACC includes drugs such as cisplatin, gemcitabine etoposide, doxorubicin or capecitabine in different combinations [26]. ACC has been shown to be sensitive to drugs causing DNA damage such as cisplatin and gemcitabine [81].

Therefore, the combination of adavosertib with these two drugs could have a synergistic effect by inhibiting the DNA-repairing process, leading to an increase in cancer cells apoptosis. Interestingly we demonstrated *in vitro* a synergic effect of adavosertib with cisplatin or gemcitabine in different ACC models, including cell lines resistant to adavosertib alone. Thus, the combination of adavosertib with cisplatin or gemcitabine could represent a promising new potential option of treatment in patients with advanced ACC. The safety and efficacy of the combination treatment adavosertib with cisplatin or gemcitabine have been demonstrated in several phase I or II trials in different advanced solid tumors [128-130].

Finally, the last druggable pathway we studied, involved in ACC progression, is the FGF/FGFR pathway. This signalling regulates the development of the adrenal gland, enhances proliferation in adrenocortical cells and, if deregulated, can be regarded as a driver in the formation of many cancer types, including ACC [147]. Studies have indeed demonstrated that particularly FGFR 1 and 4 were upregulated in malignant compared to benign adrenocortical tumors and that their high expression was significantly associated with worse patient prognosis, suggesting that they are potentially interesting therapeutic targets [158, 159]. However, up to now, no single study has been published that focused on the FGF/FGFR pathway as a central mechanism that can potentially be druggable in ACC.

Our preliminary results are filling this gap, as we showed that high levels of certain FGFR receptors expression are correlating with a better response to therapy.

Our gene expression analysis revealed that FGFR-1 and FGFR-2 isoform IIIc were the most frequently expressed in ACC cell lines, even if at different levels, in line with a study demonstrating that, different from other endothelial tissues, the mesenchymal IIIc is the most expressed isoform in the adult adrenal glands [208]. The prevalence of the IIIc isoforms is related to the embryogenesis of the adrenocortical tissue, which originates from the intermediate mesoderm and undergoes to a mesenchymal–epithelial transition to result in an epithelial tissue. However, this epithelial transformation is incomplete, and the adrenal cortex keeps most of its mesenchymal characteristics at molecular level [9, 208].

Looking at FGFR4, we found the highest levels in the TVBF-7 cells, but it must point out that FGFR4 was the subtype less expressed among the others, namely FGFR 1 IIIc, FGFR2 IIIb and FGFR2 IIIc.

Concerning TVBF-7 cells, which have high expression of FGFRs, this cell line was more sensitive to the pan-FGFR-inhibitors erdafitinib and rogaratinib with an  $IC_{50}$  values close to the

targeted therapeutic ranges for unbound plasma based on efficacious concentrations in preclinical tumor models (erdafitinib >0.5 to 2.4 ng/mL) [209].

A study evaluated the antiproliferative effect of rogaratinib was assessed in a panel comprised of 66 human cancer cell lines of different histological origins and in additional cell lines reported to be sensitive to FGFR inhibition. The IC<sub>50</sub> values ranged from 27 nM to >30 μM with nine cell lines showing IC<sub>50</sub> values <1 μM. Cell proliferation inhibition was compared to available cellular FGFR expression and genomic mutation data. The sensitivity of the cell lines towards rogaratinib correlated with overall FGFR mRNA expression levels. All cell lines with a rogaratinib IC<sub>50</sub> < 1 μM showed elevated expression for at least one FGFR subtype. Cancer cell lines with a rogaratinib IC<sub>50</sub> > 1 μM either lacked overexpression of FGFRs or harbored known activating mutations and/or gene amplifications in genes described to confer resistance to FGFR inhibition, e.g., KRAS, NRAS, HRAS, PIK3CA, BRAF, PTEN or EGFR genes [210].

However, fisogatinib (BLU-554), a potent and highly selective oral FGFR4 inhibitor optimized for clinical use did not show a similar linear correlation with the FGFR4 expression, indeed, although TVBF-7 cells have a higher level of FGFR4, they didn't show more sensitivity to this drug compared to other ACC lines with lower levels of FGFR4. A phase I first-in-human trial in patients with advanced hepatocellular carcinoma (HCC) showed that fisogatinib elicited clinical responses in patients with tumor FGF19 overexpression in advanced HCC, validating the oncogenic driver role of the FGFR4 pathway in HCC and the use of FGF19 as a biomarker for patient selection [211].

Other studies have shown that it is necessary to quantify not only the FGF receptor expression but also to identify FGF/FGFR genetic alterations in order to better stratify tumor characteristic to personalize the use of FGFR inhibitors in future clinical trials and to develop effective combinations of FGF/FGFR inhibitors with other therapies [169, 212]. Thus, the challenge for the future is to also identify the underlying genetic background of the ACC in regard to FGFR gene amplifications and deletions in order to see if this plays also a role in this entity and to be able to select the right patients for the most suitable targeted FGFR inhibitors therapy. Moreover, it is necessary to test especially the FGFR inhibitors, as well as in general all drugs, on more physiological, 3D cellmodels, since this approach represents an additional step that can bridge the gap between conventional 2D monolayer cultures and animal models.

## 8. Conclusion

In conclusion, a growing knowledge of the molecular features of this malignancy as well as multidisciplinary and multi-institutional collaborative efforts have led to defining new potential druggable targets necessary to find effective novel therapies for ACC. The availability of new experimental cell models gives to researchers instruments that cover the well-known heterogeneity of this disease and have the potential to reveal so far unknown patient sub-type characteristics.

Our results give further support to the role of Pg in ACC. It is worth underlining that the Pg analogue megestrol acetate is already part of cancer supportive care, thus allowing having another pharmacological tool with a well-known risk/benefit profile over the usual systemic therapy in reducing ACC progression in patients undergoing EDP-M therapy. This hypothesis is now under study in the ongoing randomized phase II clinical trial PESETA (EudraCT Number: 2020-004530-38). Furthermore, preliminary results obtained in the ongoing projects on the WEE1 inhibitor adavosertib and FGFRs-inhibitors are encouraging to continue the studies on these new druggable targets in ACC, in order to generate robust results that will lead to potential clinical application, providing the basis for future clinical studies to evaluate the clinical efficacy of single and combined therapy in this rare disease with otherwise dismal outcome.

## 9. References

1. De Silva, D.C. and B. Wijesiriwardene, *The adrenal glands and their functions*. Ceylon Med J, 2007. **52**(3): p. 95-100.
2. Burford, N.G., N.A. Webster, and D. Cruz-Topete, *Hypothalamic-Pituitary-Adrenal Axis Modulation of Glucocorticoids in the Cardiovascular System*. Int J Mol Sci, 2017. **18**(10).
3. Kim, A.C., et al., *In search of adrenocortical stem and progenitor cells*. Endocr Rev, 2009. **30**(3): p. 241-63.
4. Lotfi, C.F.P., et al., *The human adrenal cortex: growth control and disorders*. Clinics (Sao Paulo), 2018. **73**(suppl 1): p. e473s.
5. Kanczkowski, W., M. Sue, and S.R. Bornstein, *The adrenal gland microenvironment in health, disease and during regeneration*. Hormones (Athens), 2017. **16**(3): p. 251-265.
6. Reimann, M., et al., *Adrenal medullary dysfunction as a feature of obesity*. Int J Obes (Lond), 2017. **41**(5): p. 714-721.
7. Ishimoto, H. and R.B. Jaffe, *Development and function of the human fetal adrenal cortex: a key component in the feto-placental unit*. Endocr Rev, 2011. **32**(3): p. 317-55.
8. Megha, R., et al., *Anatomy, Abdomen and Pelvis, Adrenal Glands (Suprarenal Glands)*, in *StatPearls*. 2022, StatPearls Publishing

Copyright © 2022, StatPearls Publishing LLC.: Treasure Island (FL).

9. Xing, Y., et al., *Development of adrenal cortex zonation*. Endocrinol Metab Clin North Am, 2015. **44**(2): p. 243-74.
10. Willenberg, H.S. and S.R. Bornstein, *Adrenal Cortex; Development, Anatomy, Physiology*, in *Endotext*, K.R. Feingold, et al., Editors. 2000, MDText.com, Inc.

Copyright © 2000-2022, MDText.com, Inc.: South Dartmouth (MA).

11. Keegan, C.E. and G.D. Hammer, *Recent insights into organogenesis of the adrenal cortex*. Trends Endocrinol Metab, 2002. **13**(5): p. 200-8.
12. Gallo-Payet, N., A. Martinez, and A. Lacroix, *Editorial: ACTH Action in the Adrenal Cortex: From Molecular Biology to Pathophysiology*. Front Endocrinol (Lausanne), 2017. **8**: p. 101.
13. Segawa, H., et al., *Urinary sodium/potassium ratio as a screening tool for hyperaldosteronism in men with hypertension*. Hypertens Res, 2021. **44**(9): p. 1129-1137.
14. Dutt, M., C.J. Wehrle, and I. Jialal, *Physiology, Adrenal Gland*, in *StatPearls*. 2022, StatPearls Publishing

Copyright © 2022, StatPearls Publishing LLC.: Treasure Island (FL).

15. Baranowski, E.S., W. Arlt, and J. Idkowiak, *Monogenic Disorders of Adrenal Steroidogenesis*. Horm Res Paediatr, 2018. **89**(5): p. 292-310.
16. Miller, W.L. and R.J. Auchus, *The molecular biology, biochemistry, and physiology of human steroidogenesis and its disorders*. Endocr Rev, 2011. **32**(1): p. 81-151.
17. Mete, O., et al., *Overview of the 2022 WHO Classification of Adrenal Cortical Tumors*. Endocr Pathol, 2022. **33**(1): p. 155-196.
18. Fassnacht, M., et al., *Management of adrenal incidentalomas: European Society of Endocrinology Clinical Practice Guideline in collaboration with the European Network for the Study of Adrenal Tumors*. European Journal of Endocrinology, 2016. **175**: p. G1-G34.
19. Pinto, A. and J.A. Barletta, *Adrenal Tumors in Adults*. Surg Pathol Clin, 2015. **8**(4): p. 725-49.
20. Beuschlein, F. and M. Reincke, *Adrenocortical tumorigenesis*. Ann N Y Acad Sci, 2006. **1088**: p. 319-34.
21. Putignano, P., et al., *Midnight salivary cortisol versus urinary free and midnight serum cortisol as screening tests for Cushing's syndrome*. J Clin Endocrinol Metab, 2003. **88**(9): p. 4153-7.



22. Funder, J.W., et al., *The Management of Primary Aldosteronism: Case Detection, Diagnosis, and Treatment: An Endocrine Society Clinical Practice Guideline*. J Clin Endocrinol Metab, 2016. **101**(5): p. 1889-916.
23. Tsiavos, V., et al., *A new highly sensitive and specific overnight combined screening and diagnostic test for primary aldosteronism*. Eur J Endocrinol, 2016. **175**(1): p. 21-8.
24. Mahmood, E. and C. Anastasopoulou, *Adrenal Adenoma*, in *StatPearls*. 2022, StatPearls Publishing

Copyright © 2022, StatPearls Publishing LLC.: Treasure Island (FL).

25. Fassnacht, M., et al., *European Society of Endocrinology Clinical Practice Guidelines on the management of adrenocortical carcinoma in adults, in collaboration with the European Network for the Study of Adrenal Tumors*. Eur J Endocrinol, 2018. **179**(4): p. G1-g46.
26. Fassnacht, M., et al., *Adrenocortical carcinomas and malignant pheochromocytomas: ESMO-EURACAN Clinical Practice Guidelines for diagnosis, treatment and follow-up*. Ann Oncol, 2020. **31**(11): p. 1476-1490.
27. Ribeiro, R.C. and B. Figueiredo, *Childhood adrenocortical tumours*. Eur J Cancer, 2004. **40**(8): p. 1117-26.
28. Bielinska, M., et al., *Review paper: origin and molecular pathology of adrenocortical neoplasms*. Vet Pathol, 2009. **46**(2): p. 194-210.
29. Herrmann, L.J., et al., *TP53 germline mutations in adult patients with adrenocortical carcinoma*. J Clin Endocrinol Metab, 2012. **97**(3): p. E476-85.
30. Cawood, T., et al., *Recommended evaluation of adrenal incidentalomas is costly, has high false-positive rates and confers a risk of fatal cancer that is similar to the risk of the adrenal lesion becoming malignant; time for a rethink?* European Journal of Endocrinology, 2009. **161**: p. 513-527.
31. Berruti, A., et al., *Prognostic role of overt hypercortisolism in completely operated patients with adrenocortical cancer*. European Urology, 2014. **65**: p. 832-838.
32. Else, T., et al., *Adrenocortical carcinoma*. Endocrine Reviews, 2014. **35**: p. 282-326.
33. Fassnacht, M., et al., *Adrenocortical carcinoma: a clinician's update*. Nature Reviews Endocrinology, 2011. **7**: p. 323-335.
34. Seccia, T., et al., *Aldosterone-producing adrenocortical carcinoma: an unusual cause of Conn's syndrome with an ominous clinical course*. Endocrine-Related Cancer, 2005. **12**: p. 149-159.
35. Grisanti, S., et al., *Molecular genotyping of adrenocortical carcinoma: a systematic analysis of published literature 2019–2021*. Current Opinion in Oncology, 2022. **34**(1): p. 19-28.
36. Gatta-Cherifi, B., et al., *Adrenal involvement in MEN1. Analysis of 715 cases from the Groupe d'etude des Tumeurs Endocrines database*. Eur J Endocrinol, 2012. **166**(2): p. 269-79.
37. Li, F.P., et al., *A cancer family syndrome in twenty-four kindreds*. Cancer Res, 1988. **48**(18): p. 5358-62.
38. Karamurzin, Y., et al., *Unusual DNA mismatch repair-deficient tumors in Lynch syndrome: a report of new cases and review of the literature*. Hum Pathol, 2012. **43**(10): p. 1677-87.
39. Weksberg, R., C. Shuman, and A.C. Smith, *Beckwith–Wiedemann syndrome*. American Journal of Medical Genetics Part C: Seminars in Medical Genetics, 2005. **137C**(1): p. 12-23.
40. Gaujoux, S., et al., *Inactivation of the APC gene is constant in adrenocortical tumors from patients with familial adenomatous polyposis but not frequent in sporadic adrenocortical cancers*. Clin Cancer Res, 2010. **16**(21): p. 5133-41.
41. Takazawa, R., et al., *Unusual double primary neoplasia: adrenocortical and ureteral carcinomas in werner syndrome*. Urol Int, 2004. **72**(2): p. 168-70.
42. Else, T., *Association of adrenocortical carcinoma with familial cancer susceptibility syndromes*. Mol Cell Endocrinol, 2012. **351**(1): p. 66-70.
43. Assié, G., et al., *Integrated genomic characterization of adrenocortical carcinoma*. Nat Genet, 2014. **46**(6): p. 607-12.
44. Lerario, A.M., A. Moraitis, and G.D. Hammer, *Genetics and epigenetics of adrenocortical tumors*. Mol Cell Endocrinol, 2014. **386**(1-2): p. 67-84.
45. Zheng, S., et al., *Comprehensive Pan-Genomic Characterization of Adrenocortical Carcinoma*. Cancer Cell, 2016. **29**(5): p. 723-736.

46. MacDonald, B.T., K. Tamai, and X. He, *Wnt/beta-catenin signaling: components, mechanisms, and diseases*. Dev Cell, 2009. **17**(1): p. 9-26.
47. Valenta, T., G. Hausmann, and K. Basler, *The many faces and functions of beta-catenin*. EMBO J, 2012. **31**(12): p. 2714-36.
48. Gaujoux, S., et al.,  *$\beta$ -catenin activation is associated with specific clinical and pathologic characteristics and a poor outcome in adrenocortical carcinoma*. Clin Cancer Res, 2011. **17**(2): p. 328-36.
49. Wasserman, J.D., G.P. Zambetti, and D. Malkin, *Towards an understanding of the role of p53 in adrenocortical carcinogenesis*. Mol Cell Endocrinol, 2012. **351**(1): p. 101-10.
50. Altieri, B., A. Colao, and A. Faggiano, *The role of insulin-like growth factor system in the adrenocortical tumors*. Minerva endocrinologica, 2019. **44**(1): p. 43-57.
51. Gicquel, C., et al., *Rearrangements at the 11p15 locus and overexpression of insulin-like growth factor-II gene in sporadic adrenocortical tumors*. J Clin Endocrinol Metab, 1994. **78**(6): p. 1444-53.
52. Weber, M.M., et al., *Insulin-like growth factor receptors in normal and tumorous adult human adrenocortical glands*. Eur J Endocrinol, 1997. **136**(3): p. 296-303.
53. Giordano, T.J., et al., *Distinct transcriptional profiles of adrenocortical tumors uncovered by DNA microarray analysis*. Am J Pathol, 2003. **162**(2): p. 521-31.
54. Gicquel, C., et al., *Molecular markers and long-term recurrences in a large cohort of patients with sporadic adrenocortical tumors*. Cancer Res, 2001. **61**(18): p. 6762-7.
55. de Fraipont, F., et al., *Gene expression profiling of human adrenocortical tumors using complementary deoxyribonucleic Acid microarrays identifies several candidate genes as markers of malignancy*. J Clin Endocrinol Metab, 2005. **90**(3): p. 1819-29.
56. Fassnacht, M., et al., *Adrenocortical carcinoma: a clinician's update*. Nat Rev Endocrinol, 2011. **7**(6): p. 323-35.
57. Velazquez-Fernandez, D., et al., *Expression profiling of adrenocortical neoplasms suggests a molecular signature of malignancy*. Surgery, 2005. **138**(6): p. 1087-94.
58. Kolomecki, K., et al., *Usefulness of VEGF, MMP-2, MMP-3 and TIMP-2 serum level evaluation in patients with adrenal tumours*. Endocr Regul, 2001. **35**(1): p. 9-16.
59. Bernard, M.H., et al., *A case report in favor of a multistep adrenocortical tumorigenesis*. J Clin Endocrinol Metab, 2003. **88**(3): p. 998-1001.
60. Kamilaris, C.D.C., F. Hannah-Shmouni, and C.A. Stratakis, *Adrenocortical tumorigenesis: Lessons from genetics*. Best Pract Res Clin Endocrinol Metab, 2020. **34**(3): p. 101428.
61. Fassnacht, M., et al., *Limited prognostic value of the 2004 International Union Against Cancer staging classification for adrenocortical carcinoma: proposal for a Revised TNM Classification*. Cancer, 2009. **115**(2): p. 243-50.
62. Erdogan, I., et al., *The Role of Surgery in the Management of Recurrent Adrenocortical Carcinoma*. The Journal of Clinical Endocrinology & Metabolism, 2013. **98**(1): p. 181-191.
63. Beuschlein, F., et al., *Major prognostic role of Ki67 in localized adrenocortical carcinoma after complete resection*. J Clin Endocrinol Metab, 2015. **100**(3): p. 841-9.
64. Berruti, A., et al., *Prognostic role of overt hypercortisolism in completely operated patients with adrenocortical cancer*. Eur Urol, 2014. **65**(4): p. 832-8.
65. Elhassan, Y.S., et al., *S-GRAS score for prognostic classification of adrenocortical carcinoma: an international, multicenter ENSAT study*. Eur J Endocrinol, 2021. **186**(1): p. 25-36.
66. Terzolo, M., et al., *Management of adrenal cancer: a 2013 update*. J Endocrinol Invest, 2014. **37**(3): p. 207-17.
67. Megerle, F., et al., *Mitotane Monotherapy in Patients With Advanced Adrenocortical Carcinoma*. J Clin Endocrinol Metab, 2018. **103**(4): p. 1686-1695.
68. Terzolo, M., et al., *Adjuvant mitotane treatment for adrenocortical carcinoma*. N Engl J Med, 2007. **356**(23): p. 2372-80.
69. Sbiera, S., et al., *Mitotane Inhibits Sterol-O-Acyl Transferase 1 Triggering Lipid-Mediated Endoplasmic Reticulum Stress and Apoptosis in Adrenocortical Carcinoma Cells*. Endocrinology, 2015. **156**(11): p. 3895-908.

70. Altieri, B., E. Lalli, and A. Faggiano, *Mitotane treatment in adrenocortical carcinoma: mechanisms of action and predictive markers of response to therapy*. *Minerva Endocrinol (Torino)*, 2022. **47**(2): p. 203-214.
71. Cremaschi, V., et al., *Advances in adrenocortical carcinoma pharmacotherapy: what is the current state of the art?* *Expert Opin Pharmacother*, 2022. **23**(12): p. 1413-1424.
72. Laganà, M., et al., *Efficacy of the EDP-M Scheme Plus Adjunctive Surgery in the Management of Patients with Advanced Adrenocortical Carcinoma: The Brescia Experience*. *Cancers (Basel)*, 2020. **12**(4).
73. Hermsen, I.G., et al., *Plasma concentrations of o,p'DDD, o,p'DDA, and o,p'DDE as predictors of tumor response to mitotane in adrenocortical carcinoma: results of a retrospective ENS@T multicenter study*. *J Clin Endocrinol Metab*, 2011. **96**(6): p. 1844-51.
74. Bates, S.E., et al., *Mitotane enhances cytotoxicity of chemotherapy in cell lines expressing a multidrug resistance gene (mdr-1/P-glycoprotein) which is also expressed by adrenocortical carcinomas*. *J Clin Endocrinol Metab*, 1991. **73**(1): p. 18-29.
75. Villa, R., et al., *Modulation of cytotoxic drug activity by mitotane and lonidamine in human adrenocortical carcinoma cells*. *Int J Oncol*, 1999. **14**(1): p. 133-8.
76. Fay, A.P., et al., *Adrenocortical carcinoma: the management of metastatic disease*. *Crit Rev Oncol Hematol*, 2014. **92**(2): p. 123-32.
77. *Cancer*. 1998. p. 2194.
78. Berruti, A., et al., *Etoposide, doxorubicin and cisplatin plus mitotane in the treatment of advanced adrenocortical carcinoma: a large prospective phase II trial*. *Endocr Relat Cancer*, 2005. **12**(3): p. 657-66.
79. Fassnacht, M., et al., *Combination chemotherapy in advanced adrenocortical carcinoma*. *N Engl J Med*, 2012. **366**(23): p. 2189-97.
80. Henning, J.E.K., et al., *Gemcitabine-Based Chemotherapy in Adrenocortical Carcinoma: A Multicenter Study of Efficacy and Predictive Factors*. *J Clin Endocrinol Metab*, 2017. **102**(11): p. 4323-4332.
81. Sperone, P., et al., *Gemcitabine plus metronomic 5-fluorouracil or capecitabine as a second-/third-line chemotherapy in advanced adrenocortical carcinoma: a multicenter phase II study*. *Endocr Relat Cancer*, 2010. **17**(2): p. 445-53.
82. Grisanti, S., et al., *Clinical Prognostic Factors in Patients With Metastatic Adrenocortical Carcinoma Treated With Second Line Gemcitabine Plus Capecitabine Chemotherapy*. *Front Endocrinol (Lausanne)*, 2021. **12**: p. 624102.
83. Altieri, B., et al., *Next-generation therapies for adrenocortical carcinoma*. *Best Pract Res Clin Endocrinol Metab*, 2020. **34**(3): p. 101434.
84. de Cremoux, P., et al., *Expression of progesterone and estradiol receptors in normal adrenal cortex, adrenocortical tumors, and primary pigmented nodular adrenocortical disease*. *Endocr Relat Cancer*, 2008. **15**(2): p. 465-74.
85. Baquedano, M.S., et al., *Identification and developmental changes of aromatase and estrogen receptor expression in prepubertal and pubertal human adrenal tissues*. *J Clin Endocrinol Metab*, 2007. **92**(6): p. 2215-22.
86. Barzon, L., et al., *Expression of aromatase and estrogen receptors in human adrenocortical tumors*. *Virchows Arch*, 2008. **452**(2): p. 181-91.
87. Medwid, S., H. Guan, and K. Yang, *Bisphenol A stimulates adrenal cortical cell proliferation via ERβ-mediated activation of the sonic hedgehog signalling pathway*. *J Steroid Biochem Mol Biol*, 2018. **178**: p. 254-262.
88. Shen, X.C., et al., *Estrogen receptor expression in adrenocortical carcinoma*. *J Zhejiang Univ Sci B*, 2009. **10**(1): p. 1-6.
89. Montanaro, D., et al., *Antiestrogens upregulate estrogen receptor beta expression and inhibit adrenocortical H295R cell proliferation*. *J Mol Endocrinol*, 2005. **35**(2): p. 245-56.
90. Rossini, E., et al., *Cytotoxic Effect of Progesterone, Tamoxifen and Their Combination in Experimental Cell Models of Human Adrenocortical Cancer*. *Front Endocrinol (Lausanne)*, 2021. **12**: p. 669426.
91. Zhao, C., K. Dahlman-Wright, and J.A. Gustafsson, *Estrogen receptor beta: an overview and update*. *Nucl Recept Signal*, 2008. **6**: p. e003.

92. Fragni, M., et al., *In vitro antitumor activity of progesterone in human adrenocortical carcinoma*. *Endocrine*, 2019. **63**(3): p. 592-601.
93. Fiorentini, C., et al., *Antisecretive and Antitumor Activity of Abiraterone Acetate in Human Adrenocortical Cancer: A Preclinical Study*. *J Clin Endocrinol Metab*, 2016. **101**(12): p. 4594-4602.
94. Katzenellenbogen, B.S. and M.J. Norman, *Multihormonal regulation of the progesterone receptor in MCF-7 human breast cancer cells: interrelationships among insulin/insulin-like growth factor-I, serum, and estrogen*. *Endocrinology*, 1990. **126**(2): p. 891-8.
95. Carlson, J.A., Jr., et al., *Tamoxifen and endometrial carcinoma: alterations in estrogen and progesterone receptors in untreated patients and combination hormonal therapy in advanced neoplasia*. *Am J Obstet Gynecol*, 1984. **149**(2): p. 149-53.
96. Abiven-Lepage, G., et al., *Adrenocortical carcinoma and pregnancy: clinical and biological features and prognosis*. *Eur J Endocrinol*, 2010. **163**(5): p. 793-800.
97. de Corbière, P., et al., *Pregnancy in Women Previously Treated for an Adrenocortical Carcinoma*. *J Clin Endocrinol Metab*, 2015. **100**(12): p. 4604-11.
98. Altinoz, M.A., et al., *Medroxyprogesterone and tamoxifen augment anti-proliferative efficacy and reduce mitochondria-toxicity of epirubicin in FM3A tumor cells in vitro*. *Cell Biol Int*, 2007. **31**(5): p. 473-81.
99. Zaino, R.J., P.G. Satyaswaroop, and R. Mortel, *Hormonal therapy of human endometrial adenocarcinoma in a nude mouse model*. *Cancer Res*, 1985. **45**(2): p. 539-41.
100. Wen, L., et al., *Effect of tamoxifen, methoxyprogesterone acetate and combined treatment on cellular proliferation and apoptosis in SKOV3/DDP cells via the regulation of vascular endothelial growth factor*. *Arch Gynecol Obstet*, 2013. **287**(5): p. 997-1004.
101. Herzog, T.J., *What is the clinical value of adding tamoxifen to progestins in the treatment [correction for treatment] of advanced or recurrent endometrial cancer?* *Gynecol Oncol*, 2004. **92**(1): p. 1-3.
102. Rossouw, J., et al., *Risks and benefits of estrogen plus progestin in healthy postmenopausal women: principal results from the Women's Health Initiative randomized controlled trial*. *Journal of the American Medical Association*, 2002. **288**: p. 321-333.
103. Lieberman, A. and L. Curtis, *In Defense of Progesterone: A Review of the Literature*. *Altern Ther Health Med*, 2017. **23**(6): p. 24-32.
104. Núñez, C., et al., *An overview of the effective combination therapies for the treatment of breast cancer*. *Biomaterials*, 2016. **97**: p. 34-50.
105. Motamed, H.R., et al., *The apoptotic effects of progesterone on breast cancer (MCF-7) and human osteosarcoma (MG-636) cells*. *Physiol Int*, 2020. **107**(3): p. 406-418.
106. Lin, J.H., et al., *Estrogen and progesterone-related gene variants and colorectal cancer risk in women*. *BMC Med Genet*, 2011. **12**: p. 78.
107. Schürmann, R., M. Cronin, and J.U. Meyer, *Estrogen plus progestin and colorectal cancer in postmenopausal women*. *N Engl J Med*, 2004. **350**(23): p. 2417-9; author reply 2417-9.
108. Simon, M.S., et al., *Estrogen plus progestin and colorectal cancer incidence and mortality*. *J Clin Oncol*, 2012. **30**(32): p. 3983-90.
109. Motylewska, E. and G. Meleń-Mucha, *Estrone and progesterone inhibit the growth of murine MC38 colon cancer line*. *J Steroid Biochem Mol Biol*, 2009. **113**(1-2): p. 75-9.
110. Kong, X., et al., *Progesterone induces cell apoptosis via the CACNA2D3/Ca<sup>2+</sup>/p38 MAPK pathway in endometrial cancer*. *Oncol Rep*, 2020. **43**(1): p. 121-132.
111. Liu, Y., et al., *Effects of estradiol and progesterone on the growth of HeLa cervical cancer cells*. *Eur Rev Med Pharmacol Sci*, 2017. **21**(17): p. 3959-3965.
112. Hong, Y., et al., *Progesterone suppresses Aβ(42)-induced neuroinflammation by enhancing autophagy in astrocytes*. *Int Immunopharmacol*, 2018. **54**: p. 336-343.
113. Kim, H.N., S.J. Lee, and J.Y. Koh, *The neurosteroids, allopregnanolone and progesterone, induce autophagy in cultured astrocytes*. *Neurochem Int*, 2012. **60**(2): p. 125-33.
114. Kim, J., et al., *Autophagy activation and neuroprotection by progesterone in the G93A-SOD1 transgenic mouse model of amyotrophic lateral sclerosis*. *Neurobiol Dis*, 2013. **59**: p. 80-5.

115. Godbole, M., et al., *Progesterone suppresses the invasion and migration of breast cancer cells irrespective of their progesterone receptor status - a short report*. Cell Oncol (Dordr), 2017. **40**(4): p. 411-417.
116. Lima, M.A., et al., *Progesterone decreases ovarian cancer cells migration and invasion*. Steroids, 2020. **161**: p. 108680.
117. Waheed, S., et al., *Progesterone and calcitriol reduce invasive potential of endometrial cancer cells by targeting ARF6, NEDD9 and MT1-MMP*. Oncotarget, 2017. **8**(69): p. 113583-113597.
118. Abate, A., et al., *Ribociclib Cytotoxicity Alone or Combined With Progesterone and/or Mitotane in in Vitro Adrenocortical Carcinoma Cells*. Endocrinology, 2022. **163**(2).
119. Ghelli Luserna di Rorà, A., et al., *A WEE1 family business: regulation of mitosis, cancer progression, and therapeutic target*. J Hematol Oncol, 2020. **13**(1): p. 126.
120. Leijen, S., et al., *Phase I Study Evaluating WEE1 Inhibitor AZD1775 As Monotherapy and in Combination With Gemcitabine, Cisplatin, or Carboplatin in Patients With Advanced Solid Tumors*. J Clin Oncol, 2016. **34**(36): p. 4371-4380.
121. Moiseeva, T.N., et al., *WEE1 kinase inhibitor AZD1775 induces CDK1 kinase-dependent origin firing in unperturbed G1- and S-phase cells*. Proc Natl Acad Sci U S A, 2019. **116**(48): p. 23891-23893.
122. Méndez, E., et al., *A Phase I Clinical Trial of AZD1775 in Combination with Neoadjuvant Weekly Docetaxel and Cisplatin before Definitive Therapy in Head and Neck Squamous Cell Carcinoma*. Clin Cancer Res, 2018. **24**(12): p. 2740-2748.
123. Herrmann, L.J.M., et al., *TP53 Germline Mutations in Adult Patients with Adrenocortical Carcinoma*. The Journal of Clinical Endocrinology & Metabolism, 2012. **97**(3): p. E476-E485.
124. Grisanti, S., et al., *Molecular genotyping of adrenocortical carcinoma: a systematic analysis of published literature 2019-2021*. Curr Opin Oncol, 2022. **34**(1): p. 19-28.
125. Van Linden, A.A., et al., *Inhibition of Wee1 sensitizes cancer cells to antimetabolite chemotherapeutics in vitro and in vivo, independent of p53 functionality*. Mol Cancer Ther, 2013. **12**(12): p. 2675-84.
126. Aarts, M., et al., *Forced mitotic entry of S-phase cells as a therapeutic strategy induced by inhibition of WEE1*. Cancer Discov, 2012. **2**(6): p. 524-39.
127. Hirai, H., et al., *Small-molecule inhibition of Wee1 kinase by MK-1775 selectively sensitizes p53-deficient tumor cells to DNA-damaging agents*. Mol Cancer Ther, 2009. **8**(11): p. 2992-3000.
128. Leijen, S., et al., *Phase II Study of WEE1 Inhibitor AZD1775 Plus Carboplatin in Patients With TP53-Mutated Ovarian Cancer Refractory or Resistant to First-Line Therapy Within 3 Months*. J Clin Oncol, 2016. **34**(36): p. 4354-4361.
129. Lheureux, S., et al., *A randomized double-blind placebo-controlled phase II trial comparing gemcitabine monotherapy to gemcitabine in combination with adavosertib in women with recurrent, platinum resistant epithelial ovarian cancer: A trial of the Princess Margaret, California, Chicago and Mayo Phase II Consortia*. 2019, American Society of Clinical Oncology.
130. Oza, A.M., et al., *A Biomarker-enriched, Randomized Phase II Trial of Adavosertib (AZD1775) Plus Paclitaxel and Carboplatin for Women with Platinum-sensitive TP53-mutant Ovarian Cancer*. Clin Cancer Res, 2020. **26**(18): p. 4767-4776.
131. Cuneo, K.C., et al., *Dose Escalation Trial of the Wee1 Inhibitor Adavosertib (AZD1775) in Combination With Gemcitabine and Radiation for Patients With Locally Advanced Pancreatic Cancer*. J Clin Oncol, 2019. **37**(29): p. 2643-2650.
132. Cole, K.A., et al., *Phase I Clinical Trial of the Wee1 Inhibitor Adavosertib (AZD1775) with Irinotecan in Children with Relapsed Solid Tumors: A COG Phase I Consortium Report (ADVL1312)*. Clin Cancer Res, 2020. **26**(6): p. 1213-1219.
133. Thisse, B. and C. Thisse, *Functions and regulations of fibroblast growth factor signaling during embryonic development*. Dev Biol, 2005. **287**(2): p. 390-402.
134. Turner, N. and R. Grose, *Fibroblast growth factor signalling: from development to cancer*. Nat Rev Cancer, 2010. **10**(2): p. 116-29.
135. Korc, M. and R.E. Friesel, *The role of fibroblast growth factors in tumor growth*. Curr Cancer Drug Targets, 2009. **9**(5): p. 639-51.

136. Itoh, N. and D.M. Ornitz, *Evolution of the Fgf and Fgfr gene families*. Trends Genet, 2004. **20**(11): p. 563-9.
137. Farrell, B. and A.L. Breeze, *Structure, activation and dysregulation of fibroblast growth factor receptor kinases: perspectives for clinical targeting*. Biochem Soc Trans, 2018. **46**(6): p. 1753-1770.
138. Dienstmann, R., et al., *Genomic aberrations in the FGFR pathway: opportunities for targeted therapies in solid tumors*. Ann Oncol, 2014. **25**(3): p. 552-563.
139. Ornitz, D.M. and N. Itoh, *The Fibroblast Growth Factor signaling pathway*. Wiley Interdiscip Rev Dev Biol, 2015. **4**(3): p. 215-66.
140. Eswarakumar, V.P., I. Lax, and J. Schlessinger, *Cellular signaling by fibroblast growth factor receptors*. Cytokine Growth Factor Rev, 2005. **16**(2): p. 139-49.
141. Schlessinger, J., et al., *Crystal structure of a ternary FGF-FGFR-heparin complex reveals a dual role for heparin in FGFR binding and dimerization*. Mol Cell, 2000. **6**(3): p. 743-50.
142. Haase, M., et al., *CITED2 is expressed in human adrenocortical cells and regulated by basic fibroblast growth factor*. J Endocrinol, 2007. **192**(2): p. 459-65.
143. Leng, S., et al.,  *$\beta$ -Catenin and FGFR2 regulate postnatal rosette-based adrenocortical morphogenesis*. Nat Commun, 2020. **11**(1): p. 1680.
144. Guasti, L., et al., *FGF signalling through Fgfr2 isoform IIIb regulates adrenal cortex development*. Mol Cell Endocrinol, 2013. **371**(1-2): p. 182-8.
145. Partanen, J., et al., *FGFR-4, a novel acidic fibroblast growth factor receptor with a distinct expression pattern*. Embo j, 1991. **10**(6): p. 1347-54.
146. Hughes, S.E., *Differential expression of the fibroblast growth factor receptor (FGFR) multigene family in normal human adult tissues*. J Histochem Cytochem, 1997. **45**(7): p. 1005-19.
147. Tamburello, M., et al., *FGF/FGFR signaling in adrenocortical development and tumorigenesis: novel potential therapeutic targets in adrenocortical carcinoma*. Endocrine, 2022.
148. Helsten, T., et al., *The FGFR Landscape in Cancer: Analysis of 4,853 Tumors by Next-Generation Sequencing*. Clin Cancer Res, 2016. **22**(1): p. 259-67.
149. Chen, L., et al., *Fibroblast growth factor receptor fusions in cancer: opportunities and challenges*. J Exp Clin Cancer Res, 2021. **40**(1): p. 345.
150. Ronca, R., et al., *The potential of fibroblast growth factor/fibroblast growth factor receptor signaling as a therapeutic target in tumor angiogenesis*. Expert Opin Ther Targets, 2015. **19**(10): p. 1361-77.
151. Lieu, C., et al., *Beyond VEGF: inhibition of the fibroblast growth factor pathway and antiangiogenesis*. Clin Cancer Res, 2011. **17**(19): p. 6130-9.
152. Kommalapati, A., et al., *FGFR Inhibitors in Oncology: Insight on the Management of Toxicities in Clinical Practice*. Cancers (Basel), 2021. **13**(12).
153. Assie, G., T.J. Giordano, and J. Bertherat, *Gene expression profiling in adrenocortical neoplasia*. Mol Cell Endocrinol, 2012. **351**(1): p. 111-7.
154. de Reyniès, A., et al., *Gene expression profiling reveals a new classification of adrenocortical tumors and identifies molecular predictors of malignancy and survival*. J Clin Oncol, 2009. **27**(7): p. 1108-15.
155. De Martino, M.C., et al., *Molecular screening for a personalized treatment approach in advanced adrenocortical cancer*. J Clin Endocrinol Metab, 2013. **98**(10): p. 4080-8.
156. Laurell, C., et al., *Transcriptional profiling enables molecular classification of adrenocortical tumours*. Eur J Endocrinol, 2009. **161**(1): p. 141-52.
157. West, A.N., et al., *Gene expression profiling of childhood adrenocortical tumors*. Cancer Res, 2007. **67**(2): p. 600-8.
158. Brito, L.P., et al., *The role of fibroblast growth factor receptor 4 overexpression and gene amplification as prognostic markers in pediatric and adult adrenocortical tumors*. Endocr Relat Cancer, 2012. **19**(3): p. L11-3.
159. Sbiera, I., et al., *Role of FGF Receptors and Their Pathways in Adrenocortical Tumors and Possible Therapeutic Implications*. Front Endocrinol (Lausanne), 2021. **12**: p. 795116.
160. Krejci, P., et al., *Receptor tyrosine kinases activate canonical WNT/ $\beta$ -catenin signaling via MAP kinase/LRP6 pathway and direct  $\beta$ -catenin phosphorylation*. PLoS One, 2012. **7**(4): p. e35826.

161. Juhlin, C.C., et al., *Whole-Exome Sequencing Characterizes the Landscape of Somatic Mutations and Copy Number Alterations in Adrenocortical Carcinoma*. The Journal of Clinical Endocrinology & Metabolism, 2015. **100**(3): p. E493-E502.
162. Haase, M., et al., *Subcellular localization of fibroblast growth factor receptor type 2 and correlation with CTNNB1 genotype in adrenocortical carcinoma*. BMC Res Notes, 2020. **13**(1): p. 282.
163. Krook, M.A., et al., *Fibroblast growth factor receptors in cancer: genetic alterations, diagnostics, therapeutic targets and mechanisms of resistance*. Br J Cancer, 2021. **124**(5): p. 880-892.
164. Dieci, M.V., et al., *Fibroblast growth factor receptor inhibitors as a cancer treatment: from a biologic rationale to medical perspectives*. Cancer Discov, 2013. **3**(3): p. 264-79.
165. Chae, Y.K., et al., *Inhibition of the fibroblast growth factor receptor (FGFR) pathway: the current landscape and barriers to clinical application*. Oncotarget, 2017. **8**(9): p. 16052-16074.
166. Konda, B. and L.S. Kirschner, *Novel targeted therapies in adrenocortical carcinoma*. Curr Opin Endocrinol Diabetes Obes, 2016. **23**(3): p. 233-41.
167. García-Donas, J., et al., *Phase II study of dovitinib in first line metastatic or (non resectable primary) adrenocortical carcinoma (ACC): SOGUG study 2011-03*. 2014, American Society of Clinical Oncology.
168. Papadopoulos, K.P., et al., *A Phase 1 study of ARQ 087, an oral pan-FGFR inhibitor in patients with advanced solid tumours*. Br J Cancer, 2017. **117**(11): p. 1592-1599.
169. Katoh, M., *FGFR inhibitors: Effects on cancer cells, tumor microenvironment and whole-body homeostasis (Review)*. Int J Mol Med, 2016. **38**(1): p. 3-15.
170. Grisanti, S., et al., *Are we failing in treatment of adrenocortical carcinoma? Lights and shadows of molecular signatures*. Current Opinion in Endocrine and Metabolic Research, 2019. **8**: p. 80-87.
171. Rainey, W.E., K. Saner, and B.P. Schimmer, *Adrenocortical cell lines*. Mol Cell Endocrinol, 2004. **228**(1-2): p. 23-38.
172. Hantel, C., et al., *Targeting heterogeneity of adrenocortical carcinoma: Evaluation and extension of preclinical tumor models to improve clinical translation*. Oncotarget, 2016. **7**(48): p. 79292-79304.
173. Kiseljak-Vassiliades, K., et al., *Development of new preclinical models to advance adrenocortical carcinoma research*. Endocr Relat Cancer, 2018. **25**(4): p. 437-451.
174. Landwehr, L.S., et al., *A novel patient-derived cell line of adrenocortical carcinoma shows a pathogenic role of germline MUTYH mutation and high tumour mutational burden*. Eur J Endocrinol, 2021. **184**(6): p. 823-835.
175. Sigala, S., et al., *A Comprehensive Investigation of Steroidogenic Signaling in Classical and New Experimental Cell Models of Adrenocortical Carcinoma*. Cells, 2022. **11**(9).
176. Sigala, S., et al., *An update on adrenocortical cell lines of human origin*. Endocrine, 2022.
177. Chou, T.C. and P. Talalay, *Quantitative analysis of dose-effect relationships: the combined effects of multiple drugs or enzyme inhibitors*. Adv Enzyme Regul, 1984. **22**: p. 27-55.
178. Klöppel, G., et al., *Who classification of tumours of endocrine organs*. Lyon, France: World Health Organization, 2017.
179. Lippert, J., et al., *Targeted Molecular Analysis in Adrenocortical Carcinomas: A Strategy Toward Improved Personalized Prognostication*. J Clin Endocrinol Metab, 2018. **103**(12): p. 4511-4523.
180. Altieri, B., et al., *Livin/BIRC7 expression as malignancy marker in adrenocortical tumors*. Oncotarget, 2017. **8**(6): p. 9323-9338.
181. Fiorentini, C., et al., *GPNMB/OA protein increases the invasiveness of human metastatic prostate cancer cell lines DU145 and PC3 through MMP-2 and MMP-9 activity*. Exp Cell Res, 2014. **323**(1): p. 100-111.
182. González-Polo, R.A., et al., *The apoptosis/autophagy paradox: autophagic vacuolization before apoptotic death*. J Cell Sci, 2005. **118**(Pt 14): p. 3091-102.
183. Cabral-Pacheco, G.A., et al., *The Roles of Matrix Metalloproteinases and Their Inhibitors in Human Diseases*. Int J Mol Sci, 2020. **21**(24).
184. Volante, M., et al., *Matrix metalloproteinase type 2 expression in malignant adrenocortical tumors: Diagnostic and prognostic significance in a series of 50 adrenocortical carcinomas*. Mod Pathol, 2006. **19**(12): p. 1563-9.
185. Carrassa, L. and G. Damia, *DNA damage response inhibitors: Mechanisms and potential applications in cancer therapy*. Cancer Treat Rev, 2017. **60**: p. 139-151.

186. Matheson, C.J., D.S. Backos, and P. Reigan, *Targeting WEE1 Kinase in Cancer*. Trends Pharmacol Sci, 2016. **37**(10): p. 872-881.
187. Truong, T.H. and C.A. Lange, *Deciphering Steroid Receptor Crosstalk in Hormone-Driven Cancers*. Endocrinology, 2018. **159**(12): p. 3897-3907.
188. Bothou, C., et al., *Novel Insights into the Molecular Regulation of Ribonucleotide Reductase in Adrenocortical Carcinoma Treatment*. Cancers (Basel), 2021. **13**(16).
189. Huang, X., et al., *Tauroursodeoxycholic acid mediates endoplasmic reticulum stress and autophagy in adrenocortical carcinoma cells*. Oncol Lett, 2019. **18**(6): p. 6475-6482.
190. Sousa, D., S.S. Pereira, and D. Pignatelli, *Modulation of Autophagy in Adrenal Tumors*. Front Endocrinol (Lausanne), 2022. **13**: p. 937367.
191. Tompkins, K., et al., *SAT-LB064 Mitotane Induces Autophagy: A Mechanism to Promote Chemoresistance in Adrenocortical Carcinoma*. Journal of the Endocrine Society, 2019. **3**(Supplement\_1).
192. Yang, Z.J., et al., *Autophagy modulation for cancer therapy*. Cancer Biol Ther, 2011. **11**(2): p. 169-76.
193. Atif, F., S. Yousuf, and D.G. Stein, *Anti-tumor effects of progesterone in human glioblastoma multiforme: role of PI3K/Akt/mTOR signaling*. J Steroid Biochem Mol Biol, 2015. **146**: p. 62-73.
194. Syed, V. and S.M. Ho, *Progesterone-induced apoptosis in immortalized normal and malignant human ovarian surface epithelial cells involves enhanced expression of FasL*. Oncogene, 2003. **22**(44): p. 6883-90.
195. Fedotcheva, T.A., N.I. Fedotcheva, and N.L. Shimanovsky, *Progestins as Anticancer Drugs and Chemosensitizers, New Targets and Applications*. Pharmaceuticals, 2021. **13**(10).
196. Saha, S., S. Dey, and S. Nath, *Steroid Hormone Receptors: Links With Cell Cycle Machinery and Breast Cancer Progression*. Front Oncol, 2021. **11**: p. 620214.
197. Letrado, P., et al., *Zebrafish: Speeding Up the Cancer Drug Discovery Process*. Cancer Res, 2018. **78**(21): p. 6048-6058.
198. Berruti, A., et al., *Morbidity and mortality of bone metastases in advanced adrenocortical carcinoma: a multicenter retrospective study*. Eur J Endocrinol, 2019. **180**(5): p. 311-320.
199. Webb, A.H., et al., *Inhibition of MMP-2 and MMP-9 decreases cellular migration, and angiogenesis in in vitro models of retinoblastoma*. BMC Cancer, 2017. **17**(1): p. 434.
200. Asquith, C.R.M., T. Laitinen, and M.P. East, *PKMYT1: a forgotten member of the WEE1 family*. Nat Rev Drug Discov, 2020. **19**(3): p. 157.
201. Jeong, D., et al., *Protein kinase, membrane-associated tyrosine/threonine 1 is associated with the progression of colorectal cancer*. Oncol Rep, 2018. **39**(6): p. 2829-2836.
202. Liu, Y., et al., *Systematic expression analysis of WEE family kinases reveals the importance of PKMYT1 in breast carcinogenesis*. Cell Prolif, 2020. **53**(2): p. e12741.
203. Egeland, E.V., et al., *Expression and clinical significance of Wee1 in colorectal cancer*. Tumour Biol, 2016. **37**(9): p. 12133-12140.
204. Slipicevic, A., et al., *Wee1 is a novel independent prognostic marker of poor survival in post-chemotherapy ovarian carcinoma effusions*. Gynecol Oncol, 2014. **135**(1): p. 118-24.
205. Keenan, T.E., et al., *Clinical Efficacy and Molecular Response Correlates of the WEE1 Inhibitor Adavosertib Combined with Cisplatin in Patients with Metastatic Triple-Negative Breast Cancer*. Clin Cancer Res, 2021. **27**(4): p. 983-991.
206. Ponce, R.K.M., et al., *WEE1 kinase is a therapeutic vulnerability in CIC-DUX4 undifferentiated sarcoma*. JCI Insight, 2022. **7**(6).
207. Do, K., et al., *Phase I Study of Single-Agent AZD1775 (MK-1775), a Wee1 Kinase Inhibitor, in Patients With Refractory Solid Tumors*. J Clin Oncol, 2015. **33**(30): p. 3409-15.
208. Sbiera, I., et al., *Epithelial and Mesenchymal Markers in Adrenocortical Tissues: How Mesenchymal Are Adrenocortical Tissues?* Cancers (Basel), 2021. **13**(7).
209. Tabernero, J., et al., *Pharmacokinetics (PK) of the pan-FGFR inhibitor erdafitinib in urothelial carcinoma*. Annals of Oncology, 2016. **27**: p. vi273.
210. Grünewald, S., et al., *Rogaratnib: A potent and selective pan-FGFR inhibitor with broad antitumor activity in FGFR-overexpressing preclinical cancer models*. Int J Cancer, 2019. **145**(5): p. 1346-1357.



211. Kim, R.D., et al., *First-in-Human Phase I Study of Fisogatinib (BLU-554) Validates Aberrant FGF19 Signaling as a Driver Event in Hepatocellular Carcinoma*. *Cancer Discov*, 2019. **9**(12): p. 1696-1707.
212. Ghedini, G.C., et al., *Future applications of FGF/FGFR inhibitors in cancer*. *Expert Rev Anticancer Ther*, 2018. **18**(9): p. 861-872.